



2. Fundamentals and Specialties of Synthetic Aperture Radar (SAR)

Vorlesung: **Hochauflösende Radarsysteme**

WS 2007/08,

Friedrich-Alexander-Universität Erlangen Nürnberg

Lehrstuhl für Hochfrequenztechnik

Wolfgang Keydel

DLR Oberpfaffenhofen, Institut für Hochfrequenztechnik und Radarsysteme

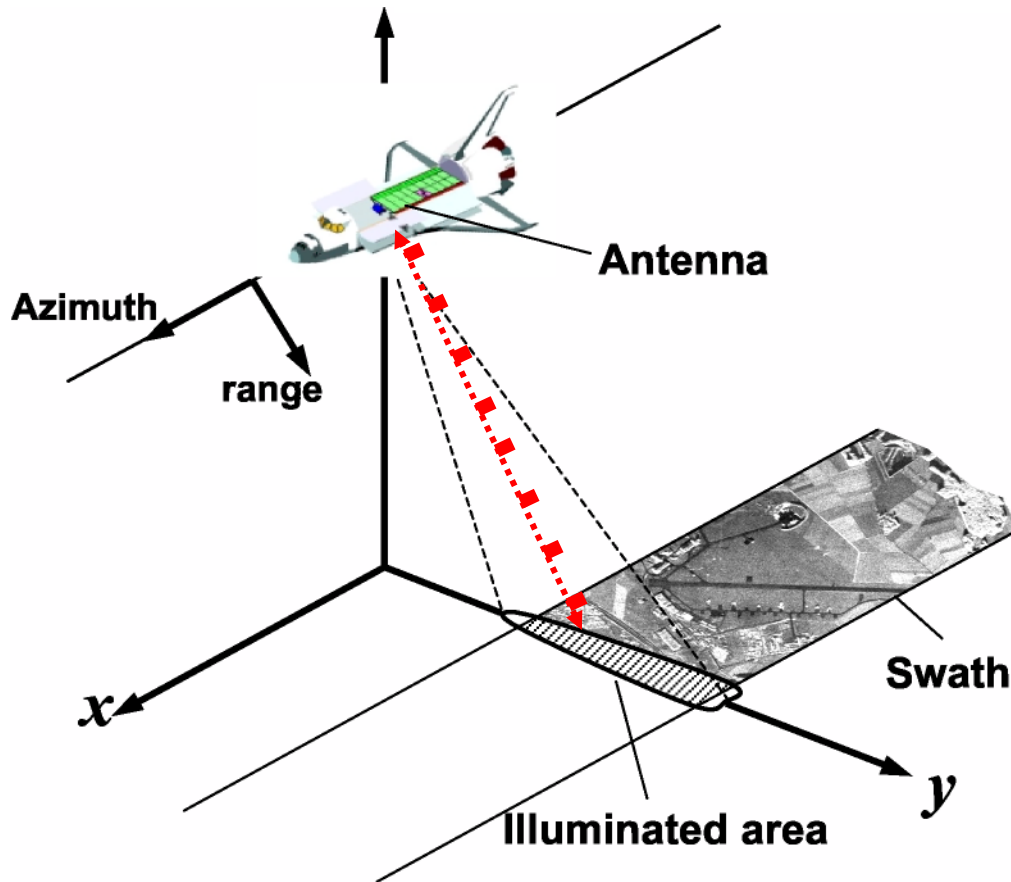
e-mail: wolfgang@keydel.com, Web: <http://www.keydel.com>

Bandwidth, B ; Puls Length, τ_P ; Range Resolution, δ_{rg}

$$B = \frac{1}{\tau_P}, \quad \delta_{rg} = \frac{c\tau_P}{2} = \frac{c}{2B}$$

τ_P	100 nsec	20 nsec	10 nsec	3,3 nsec	2 nsec	1nsec	333 psec
B	10 MHz	50 MHz	100 MHz	300MHz	500MHz	1GHz	3GHZ
δ_{rg}	15 m	3,0 m	1,5 m	0,5 m	30 cm	15 cm	5 cm

Side-Looking Imaging Geometry

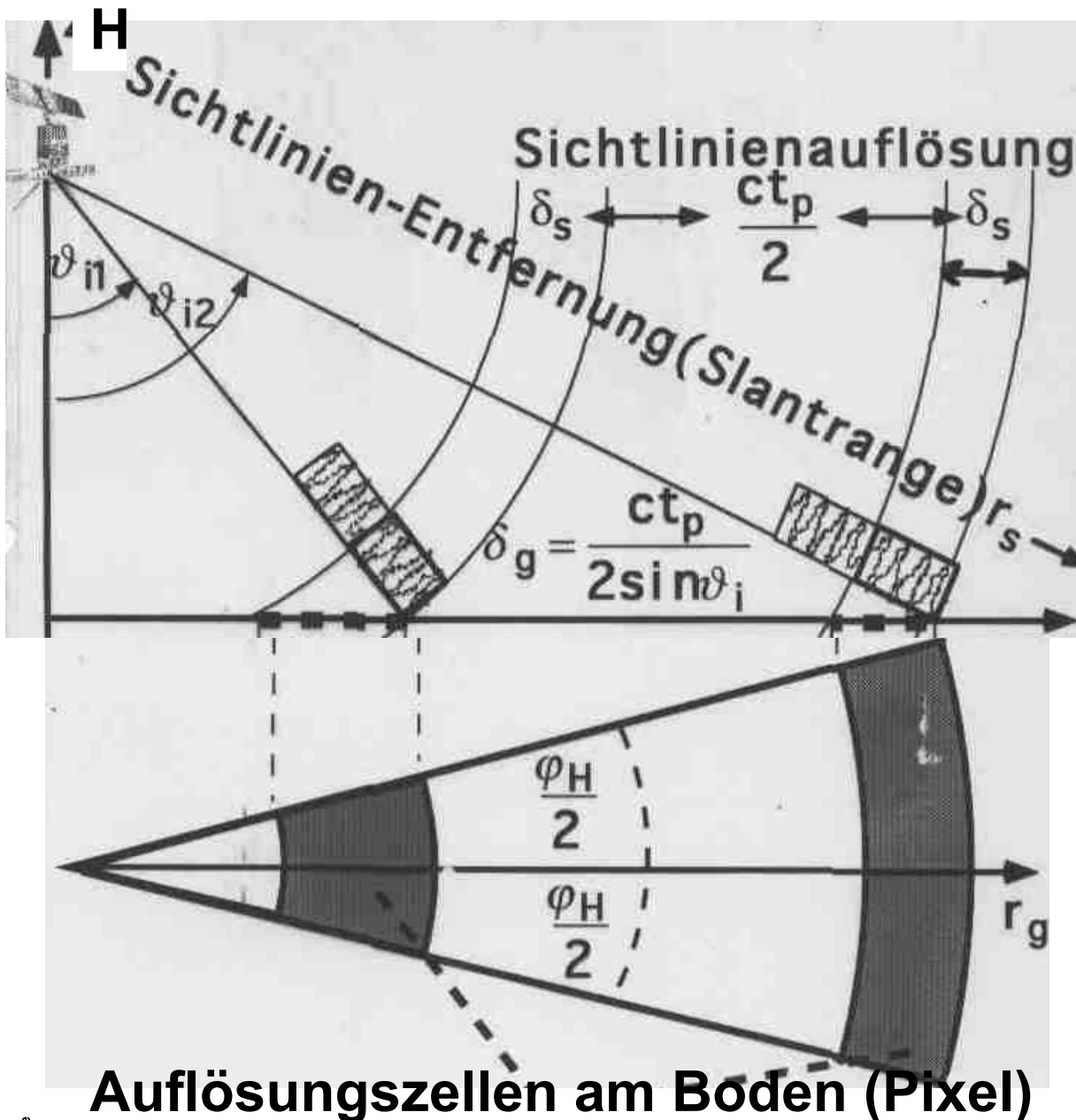


$$\frac{S}{N} = \frac{P_{ave} G^2 \lambda^2 \sigma T_D}{(4\pi)^3 r^4 (kT_0 F) L_{tot}}$$

$$\frac{S}{N} = \frac{P_{ave} G^2 \lambda^2 \sigma_0 \Delta_d \delta_{rg} T_D}{(4\pi)^3 r^4 (kT_0 F) L_{tot}}$$

$$\Delta_d = \frac{\lambda}{d} r$$

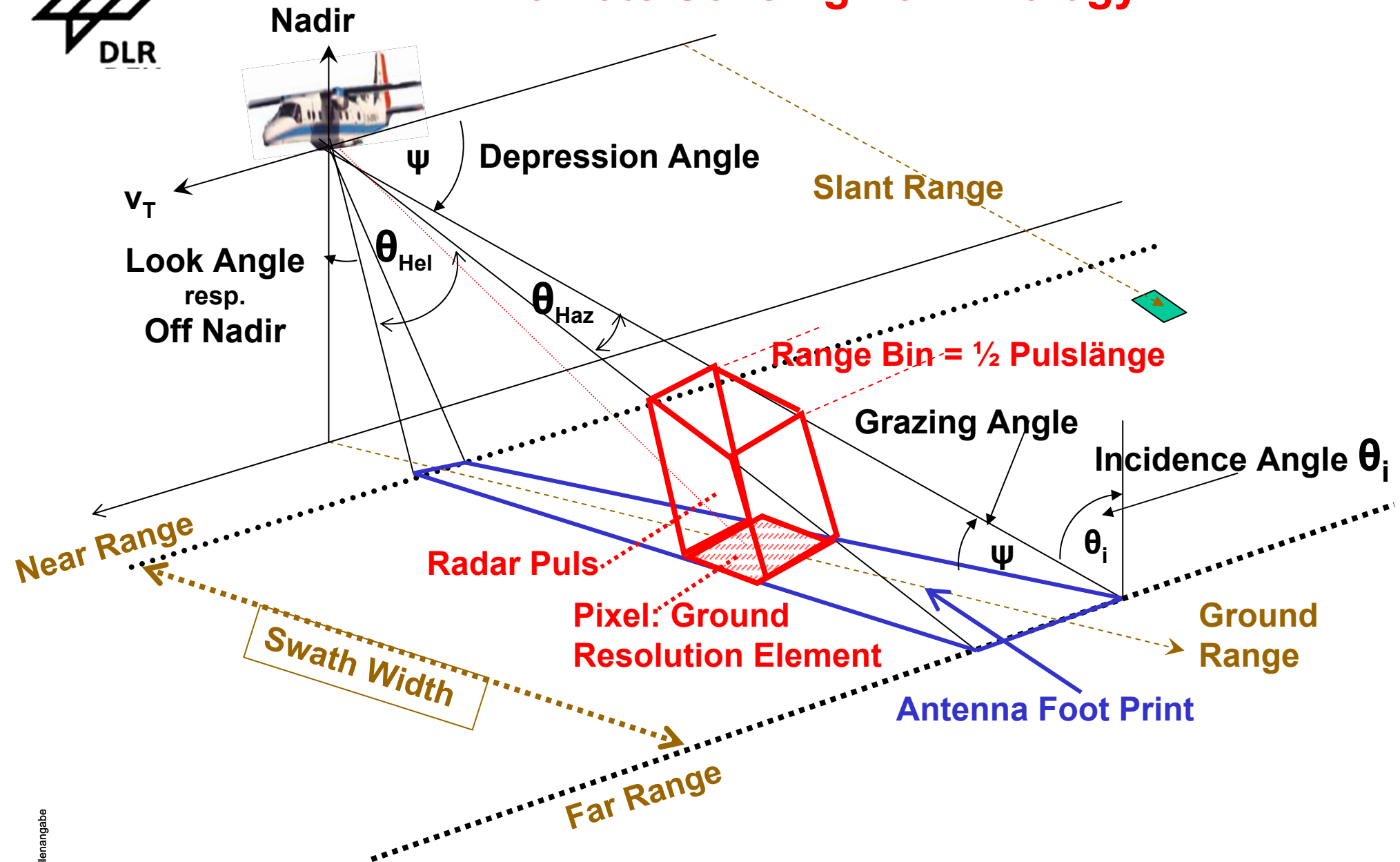
$$\frac{S}{N} = \frac{P_{ave} G^2 \lambda^3 \sigma_0 \delta_{rg} T_D}{(4\pi)^3 r^3 (kT_0 F) d L_{tot}}$$



Auflösungsgeometrie

Boden-Entfernung
Ground Range (r_g)

Remote Sensing Terminology

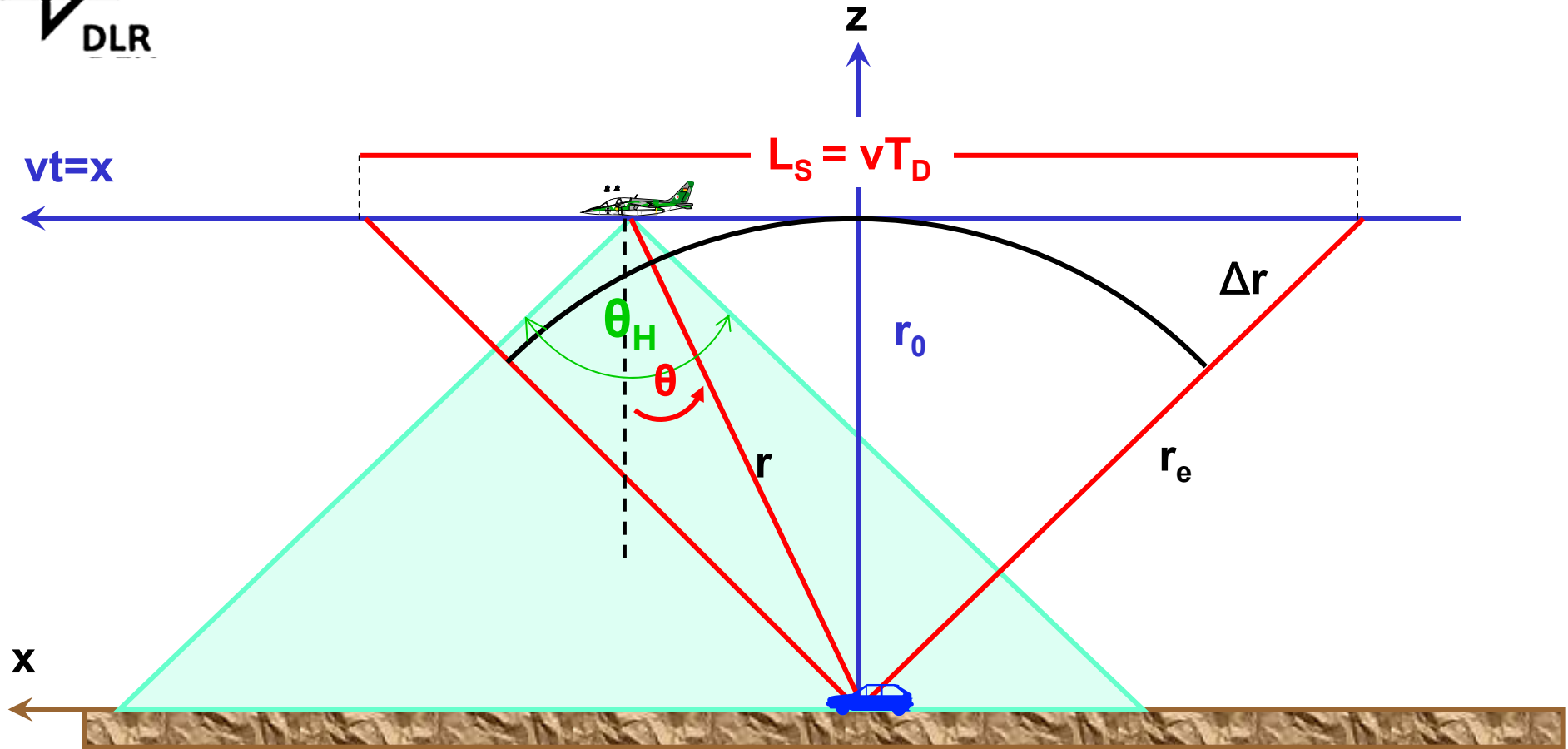


**E-SAR image (X-band) processed in real-time,
3 x 3 m resolution, 6 looks**



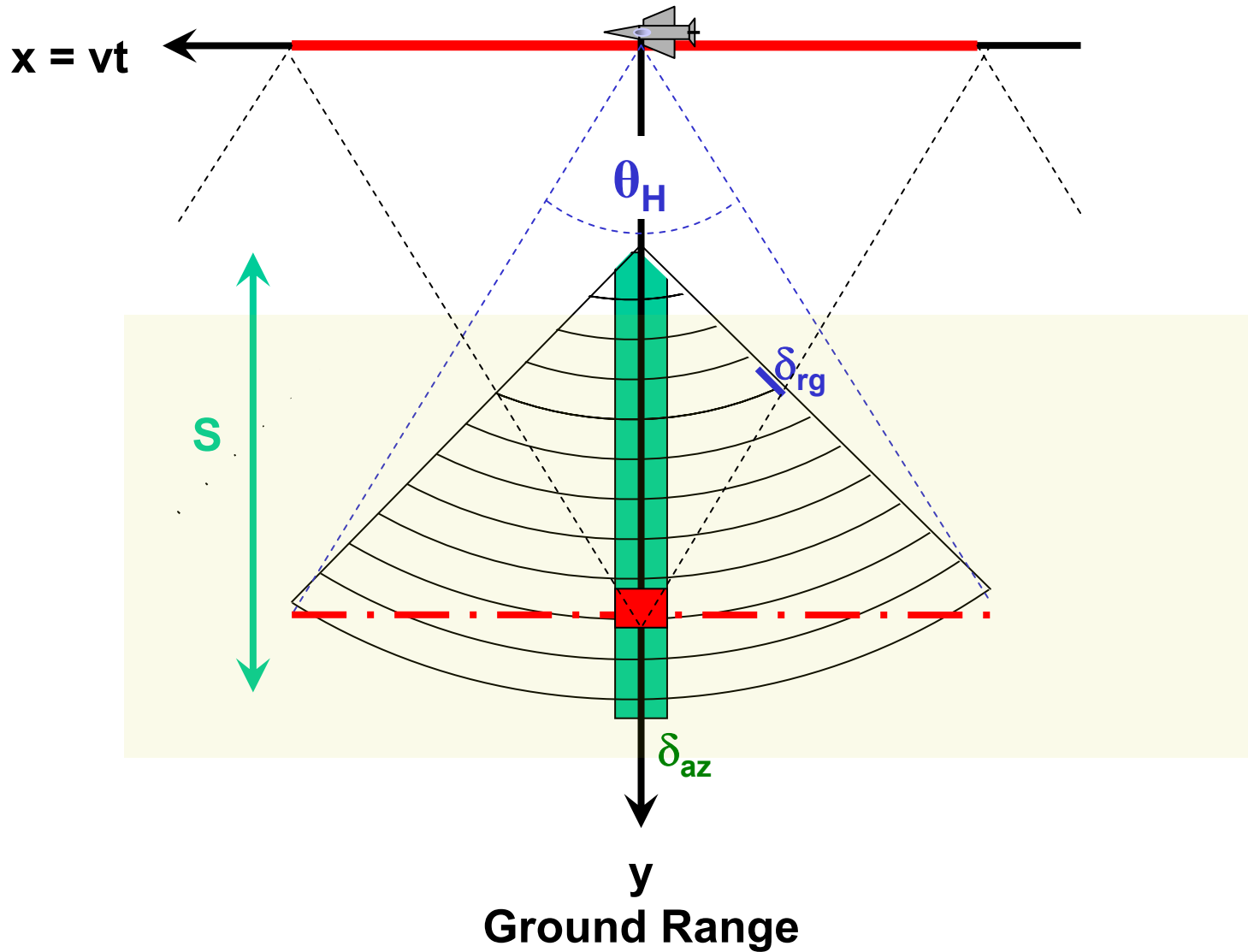
The Basic Principle of SAR

Two dimensional SAR Scheme,



Received Doppler Frequency:
$$f_D = \frac{2v}{\lambda} \sin \vartheta(t) \approx \frac{2v}{\lambda} \vartheta(t)$$

SAR Foot Print Scheme



Beam Forming with Fixed Filter $B_{\text{fix}} = \Delta f_D$

$$\Delta f_D \approx \frac{2v}{\lambda} \Delta \vartheta(t) = \frac{2v}{\lambda} \frac{\Delta x}{r} \quad \Rightarrow \quad \delta_{xDB} = \frac{\lambda}{2v} r \Delta f_D$$

Corresponding Synthetic Aperture: $L_{sDB} = \frac{2v}{\Delta f_D}$

$1/B_{\min} \leq T_{\max}$ = Time necessary to shift f_D through the whole Filter Bandwidth

$$\frac{\Delta f_D}{\Delta T} = \frac{2v}{\lambda r} \frac{\Delta x}{\Delta T} = \frac{2v^2}{\lambda r}$$

$B_{\min} = \Delta f_D$ and $T_{\max} = \Delta T$

$$\delta_{xDB} = \sqrt{\frac{r}{2\lambda}}$$

Optimum Resolution obtainable by use of a fixed Filter

Geometric SAR Azimuth Resolution

- Length of the synthetic aperture ($\Theta_a \leq 30^\circ$)

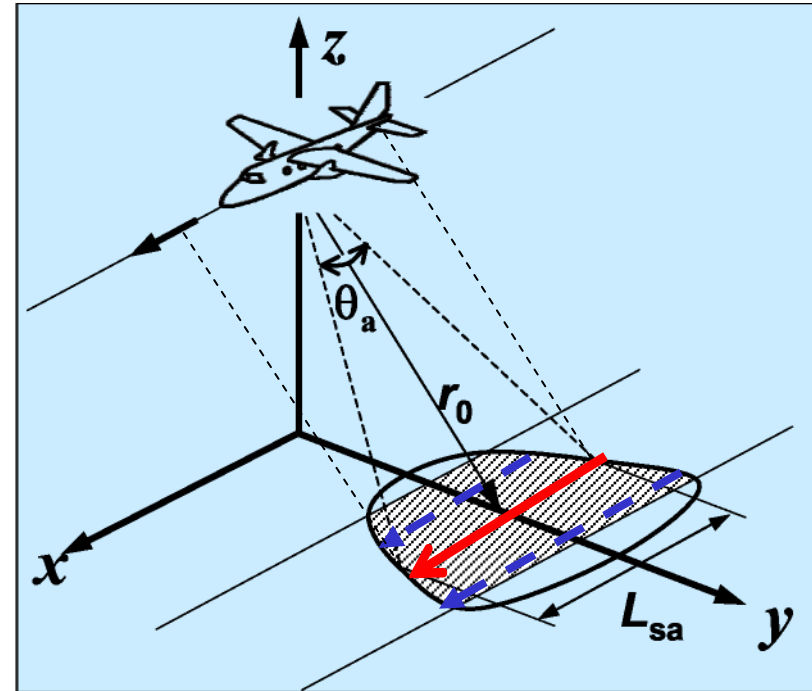
$$L_{sa} = \Theta_a \cdot r_0 = \frac{\lambda}{d_a} \cdot r_0$$

- Beam Width of the Synthetic Antenna:

$$\Theta_{sa} = d_a / 2r_0$$

Azimuth resolution

$$\delta_{sa} = d_a / 2$$



Synthetic Antenna Length = Ground Strip

Azimuth Resolution = Half Antenna Length in Azimuth



Tracking Filter leads to Matched Transmit Receive System

allows Use of **Total Dwell Time T_D** & **Largest Synthetic Aperture L_S**
SAR

$$L_S = vT_D = \frac{v}{B} \rightarrow \delta_{az} = \frac{\lambda r}{2L_S}$$

General Valid Relations (for $\theta_H \leq 30^\circ$)

$$\theta_H = \lambda/d \text{ and } L = \theta_H r$$

$$\delta_{az} = \frac{d}{2}$$

Optimum Theoretical Azimuth Resolution for Focussed SAR
(Strip Map Mode)

Synthetic Apertur Radar Basically Coherent Scatterometer

with

Very High Sophisticated Data Evaluation and Processing

**Basis: Construction of Very Large Antenna along a flight path by means of
Data Processing**

Unfocussed SAR:

neglects inherent Phase Differences with respect to a fixed Point

Azimuth Resolution (unfocussed)

$$\delta_{\text{azunfoc}} = \frac{1}{2} \sqrt{\lambda R}$$

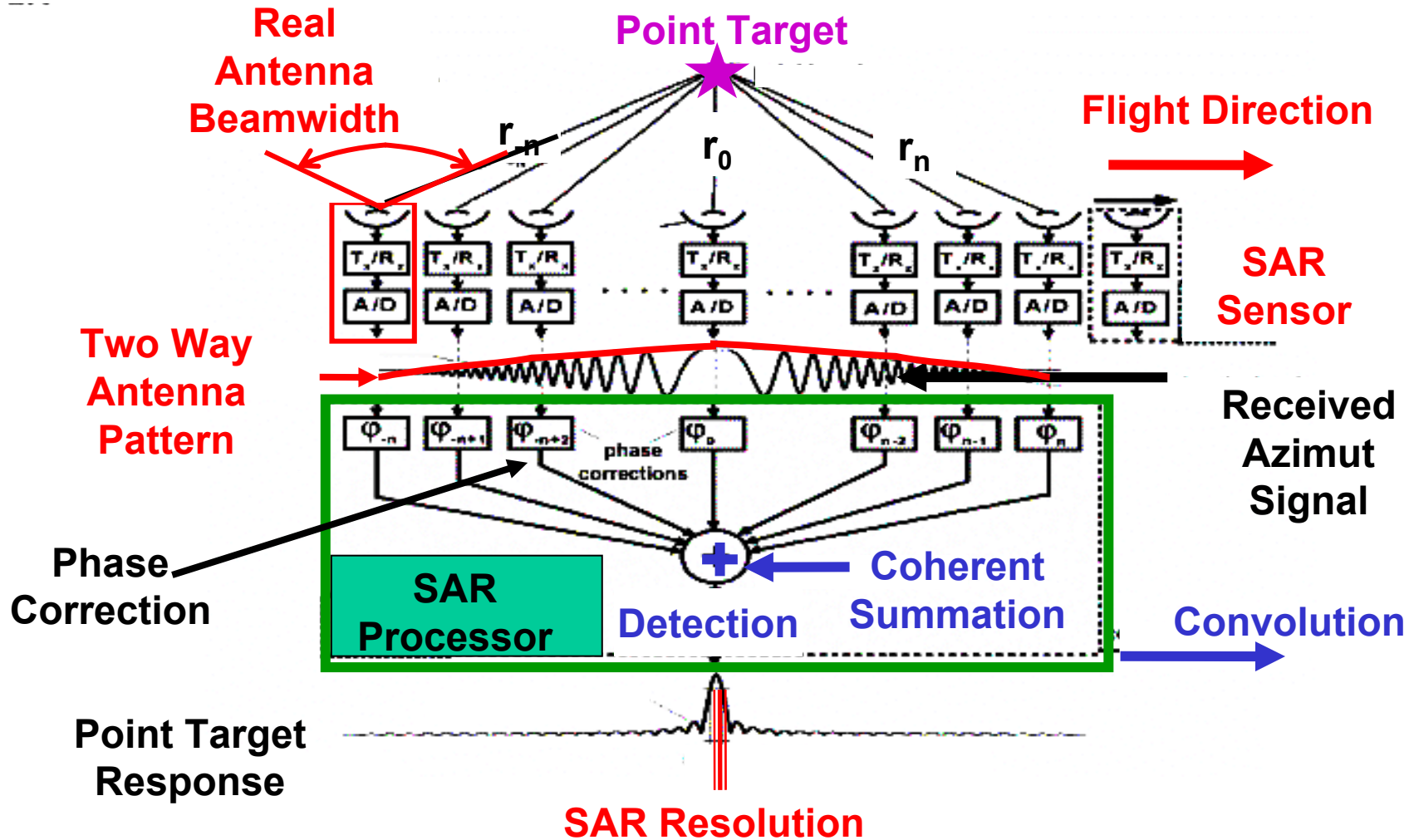
Focussed SAR:

Resolution independent of Wavelength & Distance

Azimuth Resolution

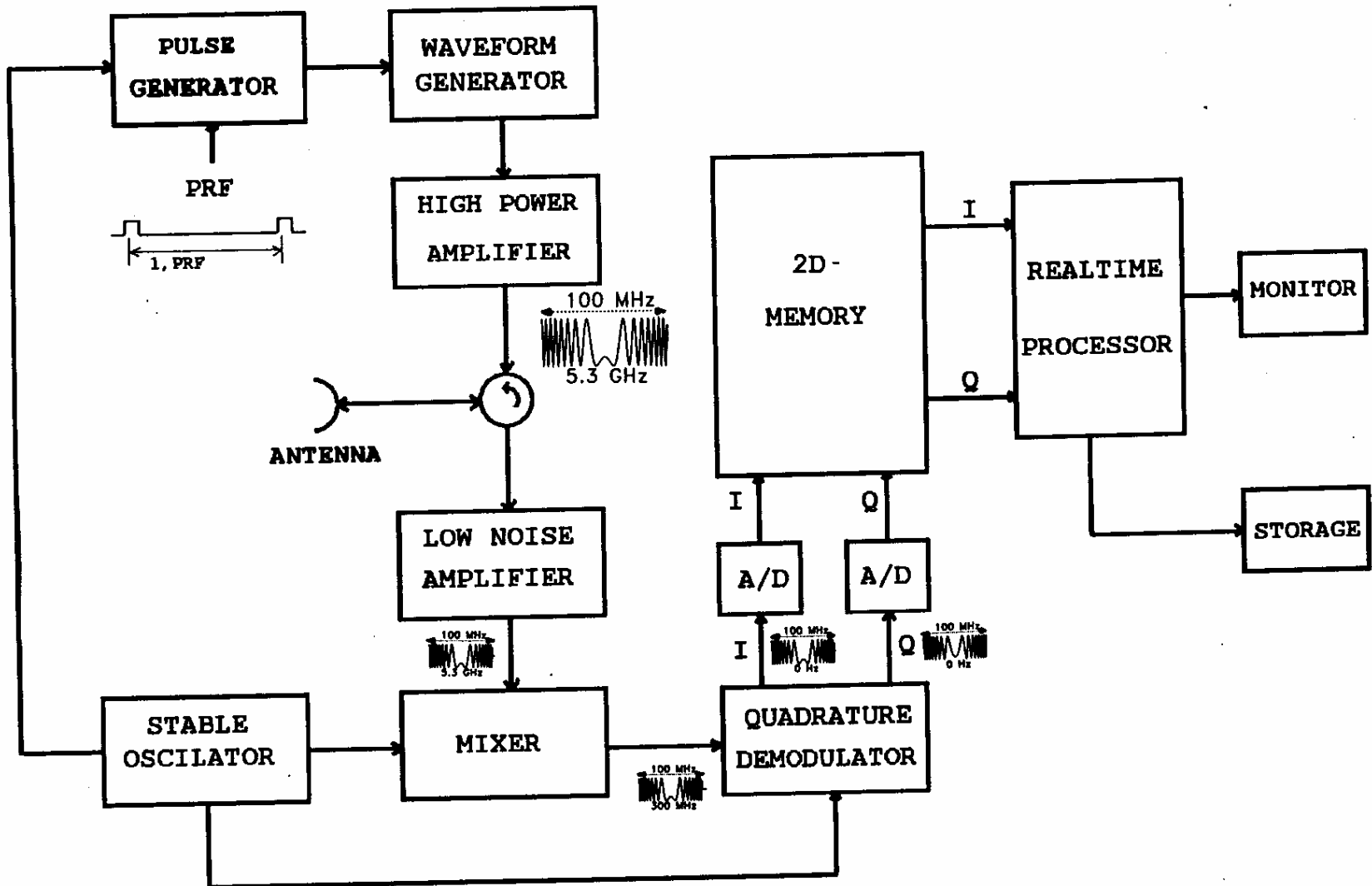
$$\delta_{\text{az}} = d/2$$

The Antenna: System Determining Element for SAR



SAR is an Antenna

SAR Block Diagramm



SAR Range Equation

Normal Radar Equation (Hall)

$$\frac{S}{N} = \frac{P_{ave} G^2 \lambda^2 \sigma T_D}{(4\pi)^3 r^4 (kT_0 F) L_{tot}}$$

$$T_D = \frac{\lambda r}{2\delta_{az} v}$$

SAR Radar Equation Point Target

$$\frac{S}{N} = \frac{P_{ave} G^2 \lambda^3 \sigma}{(4\pi)^3 r^3 (kT_0 F) 2v \delta_{az} L_{tot}}$$

$$\sigma = \sigma_o \delta_{az} \delta_{rge}$$

SAR Radar Equation Area Target

$$\frac{S}{N} = \frac{P_{ave} G^2 \lambda^3 \sigma_o \delta_{rge}}{(4\pi)^3 r^3 (kT_0 F) 2v L_{tot}}$$

All SAR Design Equations contain Antenna Parameter!!

Point Target Signal/Noise (S/N)	$S/N = \frac{P_{ave} A^2 \sigma}{(4\pi)^2 \lambda^2 R^3 (kT_0 F) 2v \delta_{az}}$
Pulse Repetition Frequency (PRF)	$2v/D \leq (PRF) \leq c/2R_{max}$
Optimum Range Resolution(δ_{rg})	$\delta_{rg} = c/2B = c\tau_p/2$
Optimum Azimuth Resolution(δ_{az})	$\delta_{az} = D/2$
Swath width(S)	$S = c D/4v$
Synthetic Aperture Length(L)	$L = \lambda R/D$
Along Track Pixel Number(N_{az})	$N_{az} = R\lambda/2\delta_{az} = L/\delta_{az}$
Across Track Pixel Number(N_{rg})	$N_{rg} = S/\delta_{rg}$
Data Rate(DR)	$DR = N_{rg} PRF$
Pixel(Sample) Rate(Q)	$Q = nvS/\delta_{az}\delta_{rg}$

A = Antenna Area, B = Bandwidth, D = Antenna Length, $kT_0 F$ = Noise Characteristic,
n = Number of Looks, P_{ave} = Mean Power, R_{max} = Maximum Distance SAR-Pixel,
v = Platform Velocity, λ = Wavelength, σ = Radar Cross Section, τ_p = Pulse Length,



SAR – RAR Comparision

Type	Point Target (S/N = SNR)	Area Target (C/N = CNR)	Contrast (S/C = SCR)
RAR	$(SNR)_{RAR} =$ $= \frac{P_{ave} G^2 \lambda^2 \sigma}{(4\pi)^3 R^4 (kT_0 F) B \tau_p (PRF) L_{tot}}$	$(SNR)_{RAR} =$ $= \frac{P_{ave} G^2 \lambda^3 \sigma_0 \delta_{rg}}{(4\pi)^3 R^3 (kT_0 F) (PRF) L_{tot}}$	$(S/N)_{RAR} = \frac{\sigma d}{\sigma_0 r \lambda B \tau_p \delta_{rg}}$
SAR	$(SNR)_{SAR} =$ $= \frac{P_{ave} G^2 \lambda^2 \sigma}{(4\pi)^3 R^3 (kT_0 F) 2v \delta_{az} L_{tot}}$	$(SNR)_{SAR} =$ $= \frac{P_{ave} G^2 \lambda^3 \sigma_0 \delta_{rg}}{(4\pi)^3 R^3 (kT_0 F) 2v L_{tot}}$	$(S/N)_{SAR} = \frac{\sigma}{\sigma_0 \delta_{rg} \delta_{az}}$
Im- prove- ment	$\frac{(SNR)_{SAR}}{(SNR)_{RAR}} = \frac{B \tau_p (PRF) \lambda r}{\delta_{rg} 2v}$	$\frac{(SNR)_{SAR}}{(SNR)_{RAR}} = \frac{(PRF) d}{2v}$	$\frac{(SCR)_{SAR}}{(SCR)_{RAR}} = \frac{B \tau_p r \lambda}{\delta_{az} d}$

Pulse Repetition Frequency

Pulse Repetition Frequency (PRF)

Dominating Factor in SAR Design

Principal Limitations:

- ★ Azimuth & Range Ambiguities
- ★ Swath Coverage- & Extension Requirements
- ★ Forbidden PRF Bands due to
 - Altitude Line Echo (ALE)
 - Altitude Variations
 - Earth Curvature & Orbit Excentricities

Lower Limit: $2vd^{-1} < PRF$

Transmitter must be pulsed before platform moves $\frac{1}{2}$ the Antenna Length d

Upper Limit

defined by Range Ambiguity Requirements

Impulse needs for crossing the Swath along r_{gmax} the Time $t_{gmax} = c (2 r_{gmax})^{-1}$

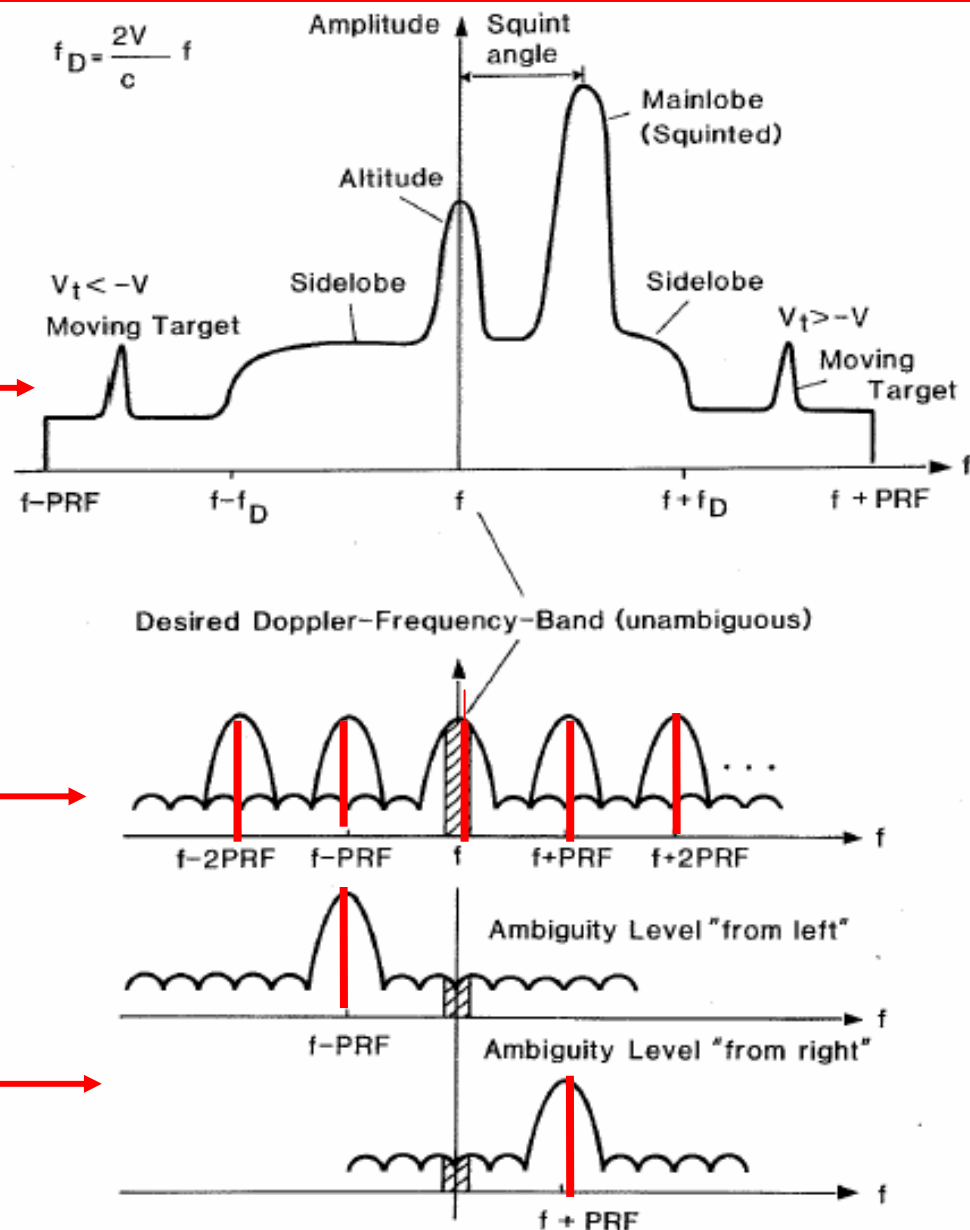
$$2 \frac{v}{d} \leq PRF \leq \frac{c}{2r_{gmax}}$$

Pulse Spectrum Scheme Moving Pulse Doppler Radar

Single Spectral Line
Fine Structure

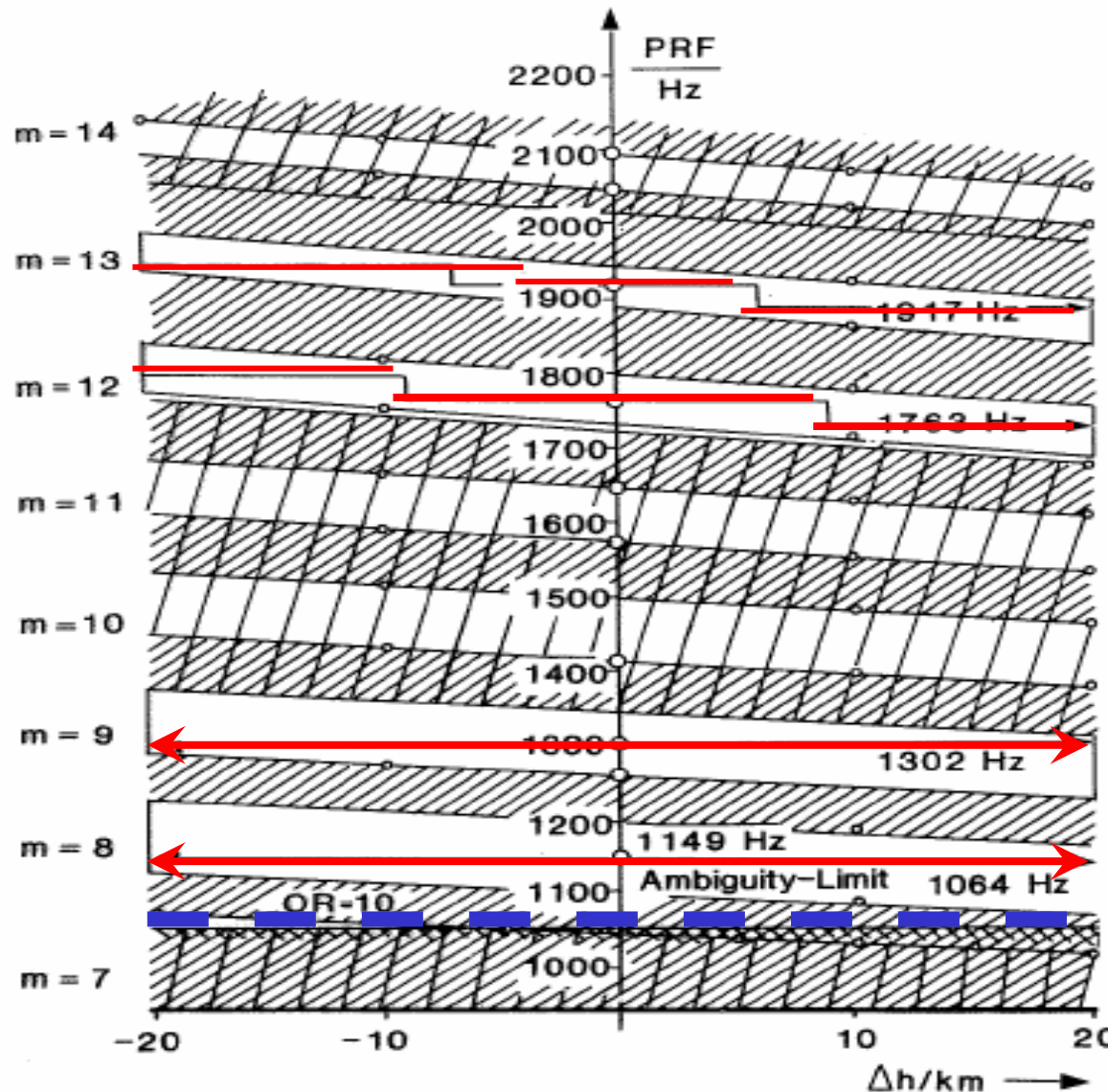
Pulse Spectrum
with
Ambiguities

Single Spectral Lines



PRF Limitations due to Altitude Variations

Allowed PRF Bands for X-Band Satellite

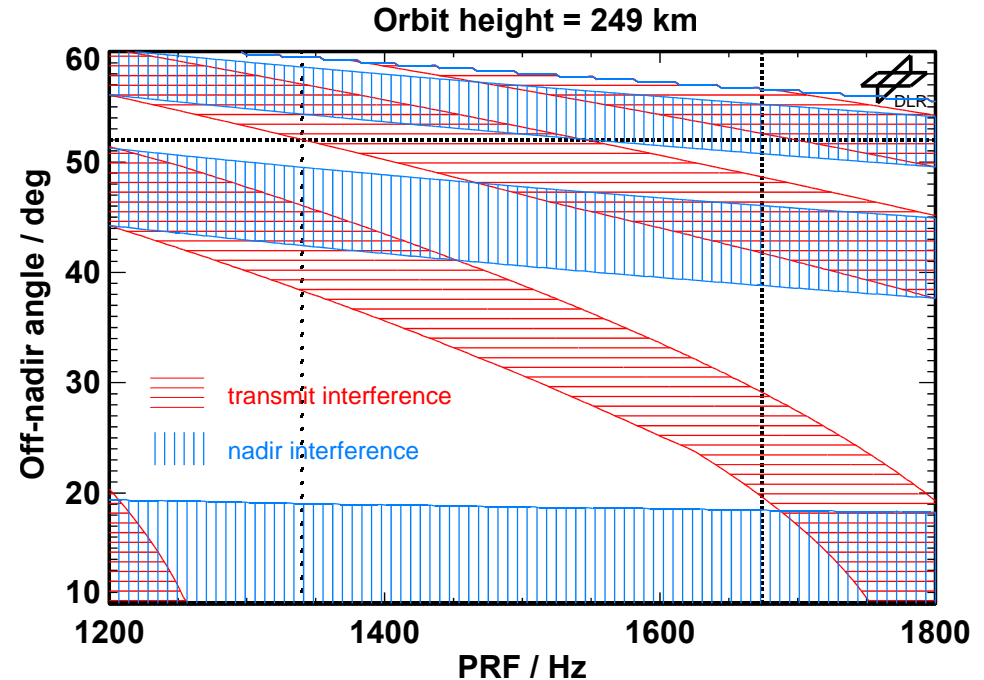
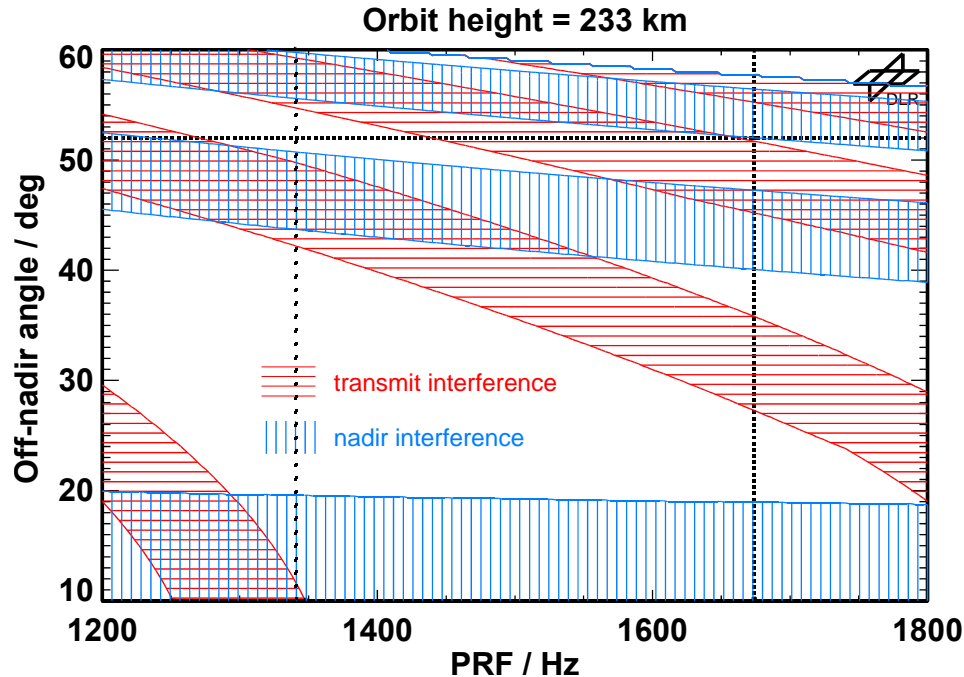


m = Number of allowed Range Ambiguities

Ambiguity Limit
1064 HZ

PRF choice for X-SAR/SRTM

Transmit & Nadir Interference Limitations

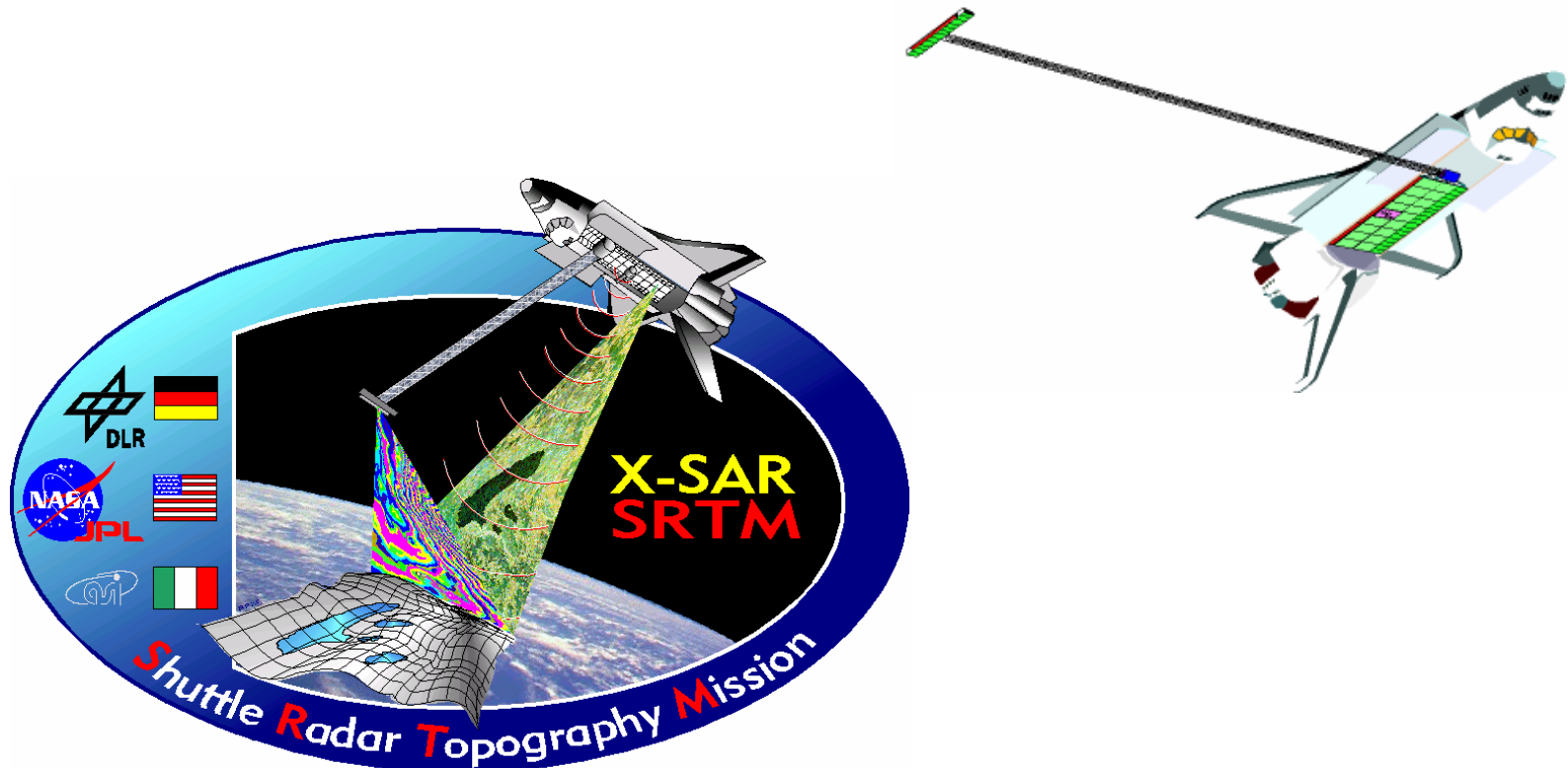


Objective: A fixed combination of PRF and Off-nadir angle

- takes into account the historical development and restrictions,
- avoid transmit and preferably nadir interferences and
- yield a good interferometric performance.

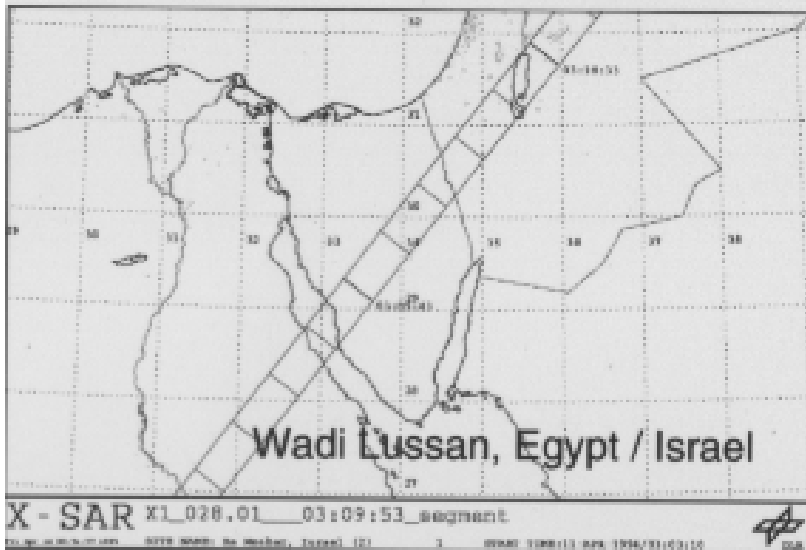
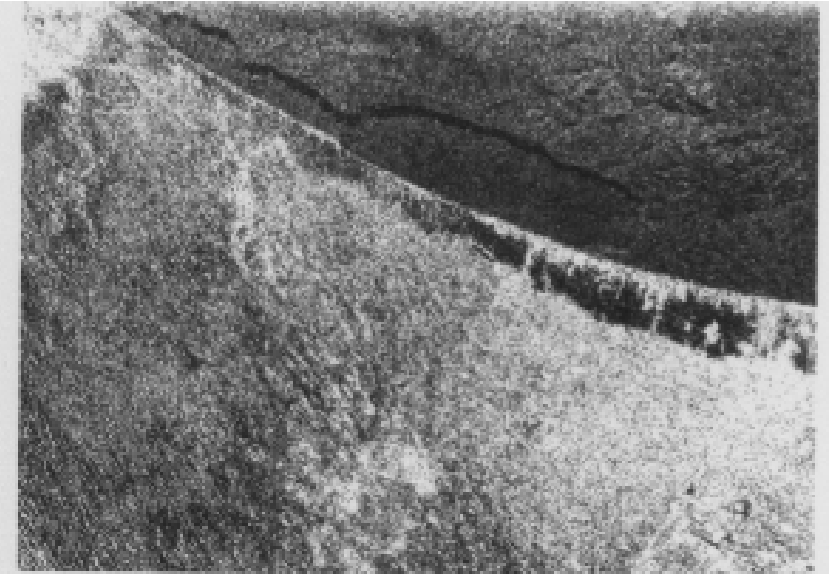
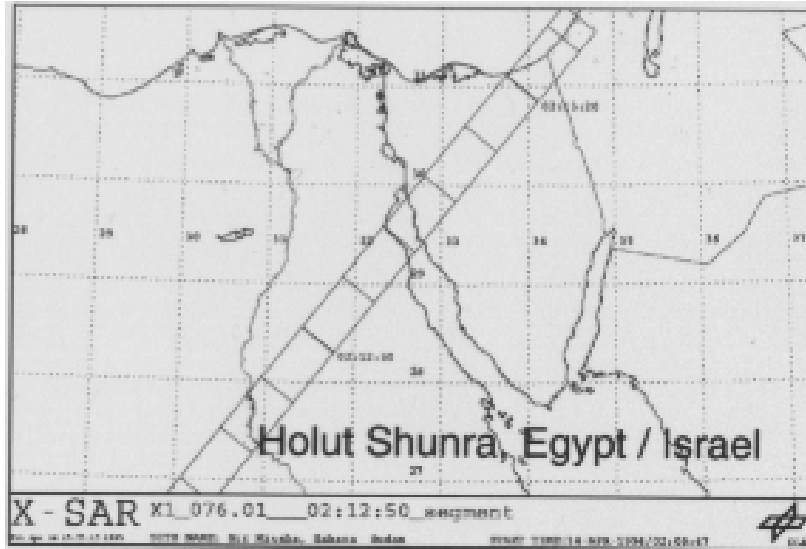
System Parameters of the X-SAR Instrument

- Orbit height from 233 km to 249 km (coverage requirement of C-Radar)
- PRF limited to eleven fixed values ranging from 1240 Hz up to 1736 Hz
- Off-nadir angle $> 51^\circ$ to avoid interference with Attitude and Orbit Determination Avionics (AODA)

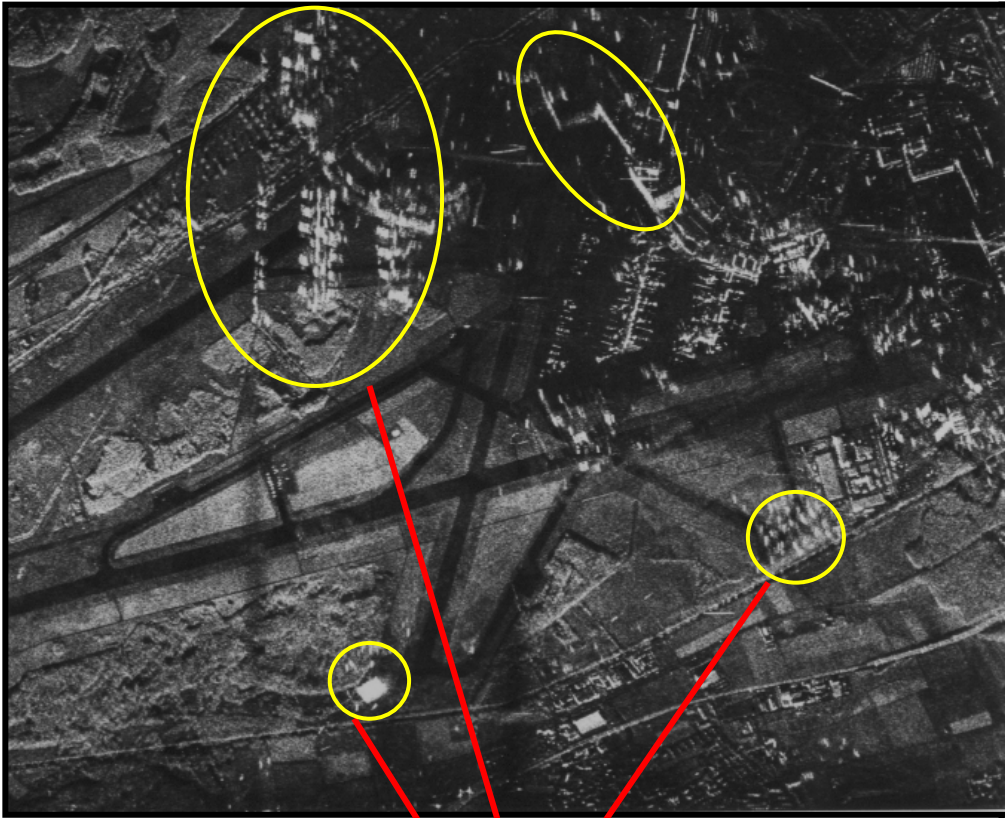


Ambiguities

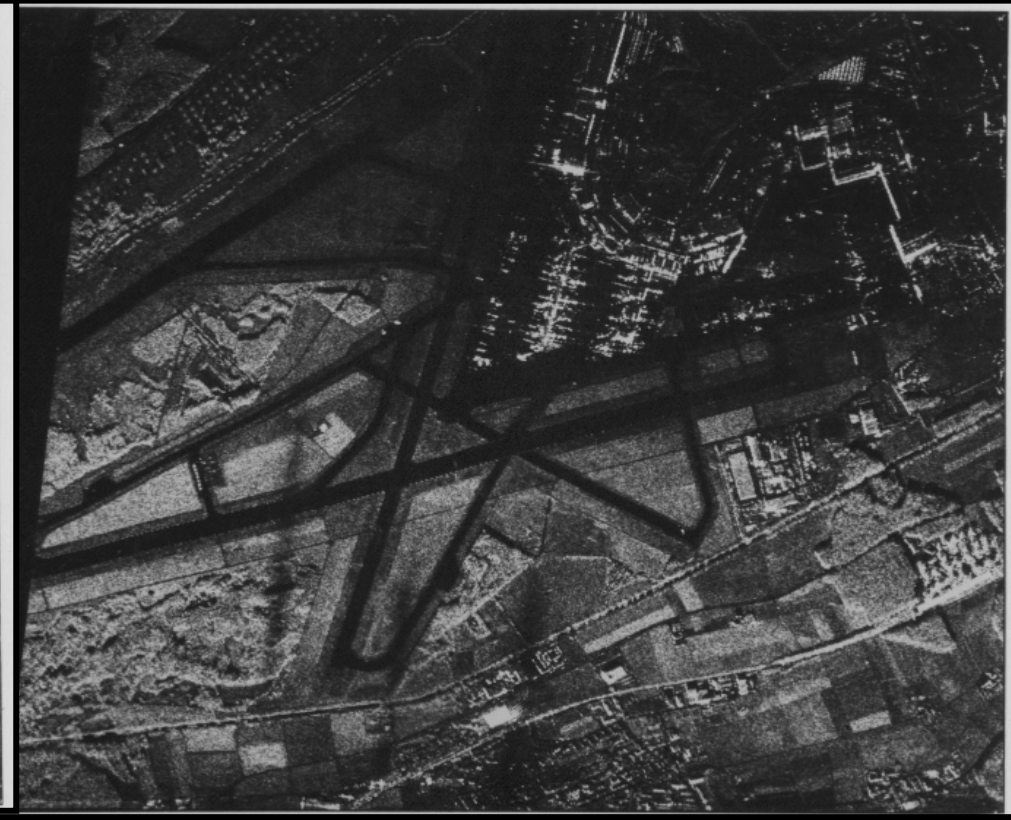
X-SAR Ambiguities



Airport Zürich Kloten with & without Ambiguities caused by 6,8° Antenna Squint Angle



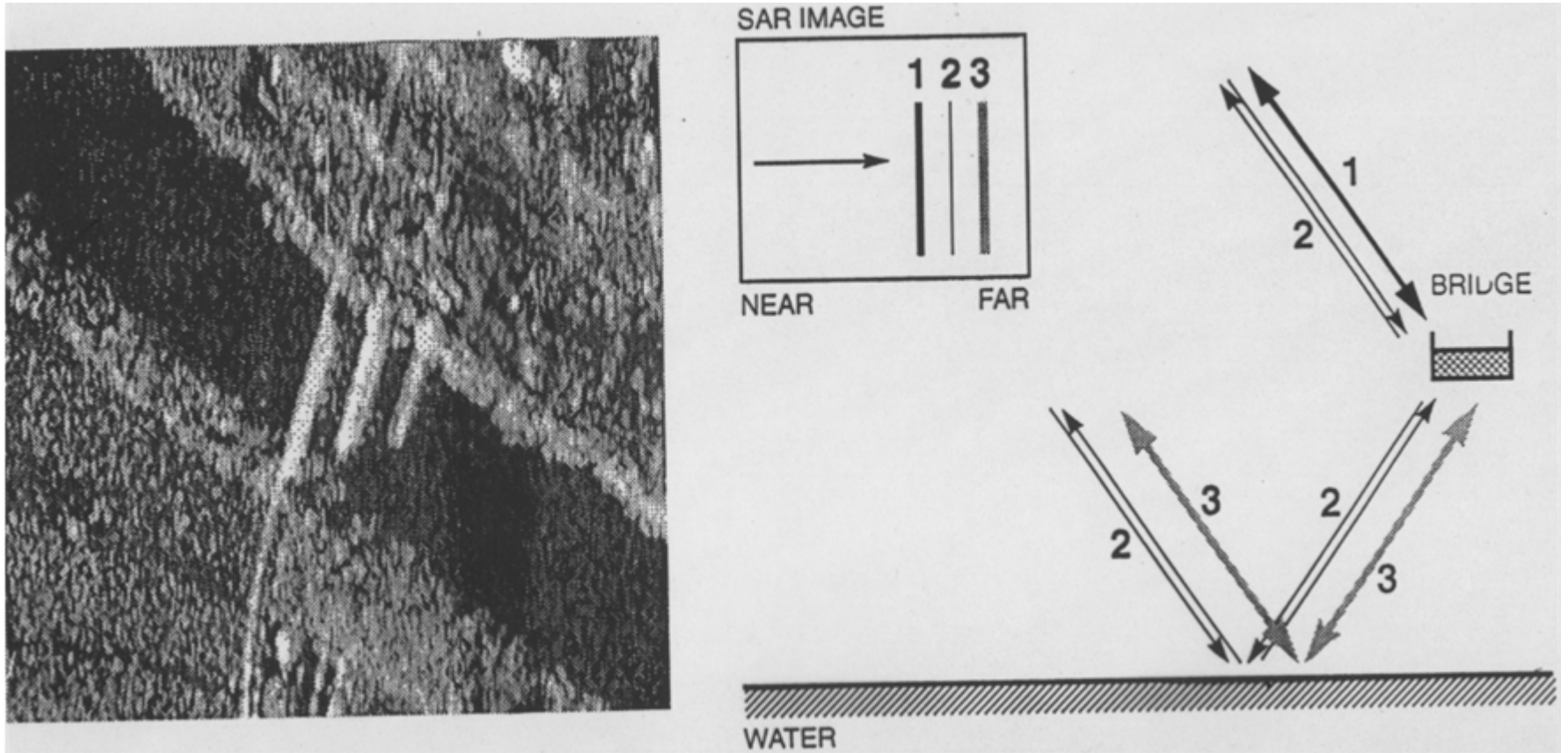
Ambiguities



E-SAR, X-VV, $\theta_{HH} = 12^\circ$, $v = 70 \text{ msec}^{-1}$

Near Range 2805m, Far Range 5355m

Ambiguities due to Multipath Reflection (Bridge)





Stripmap image
3 m azimuth resolution

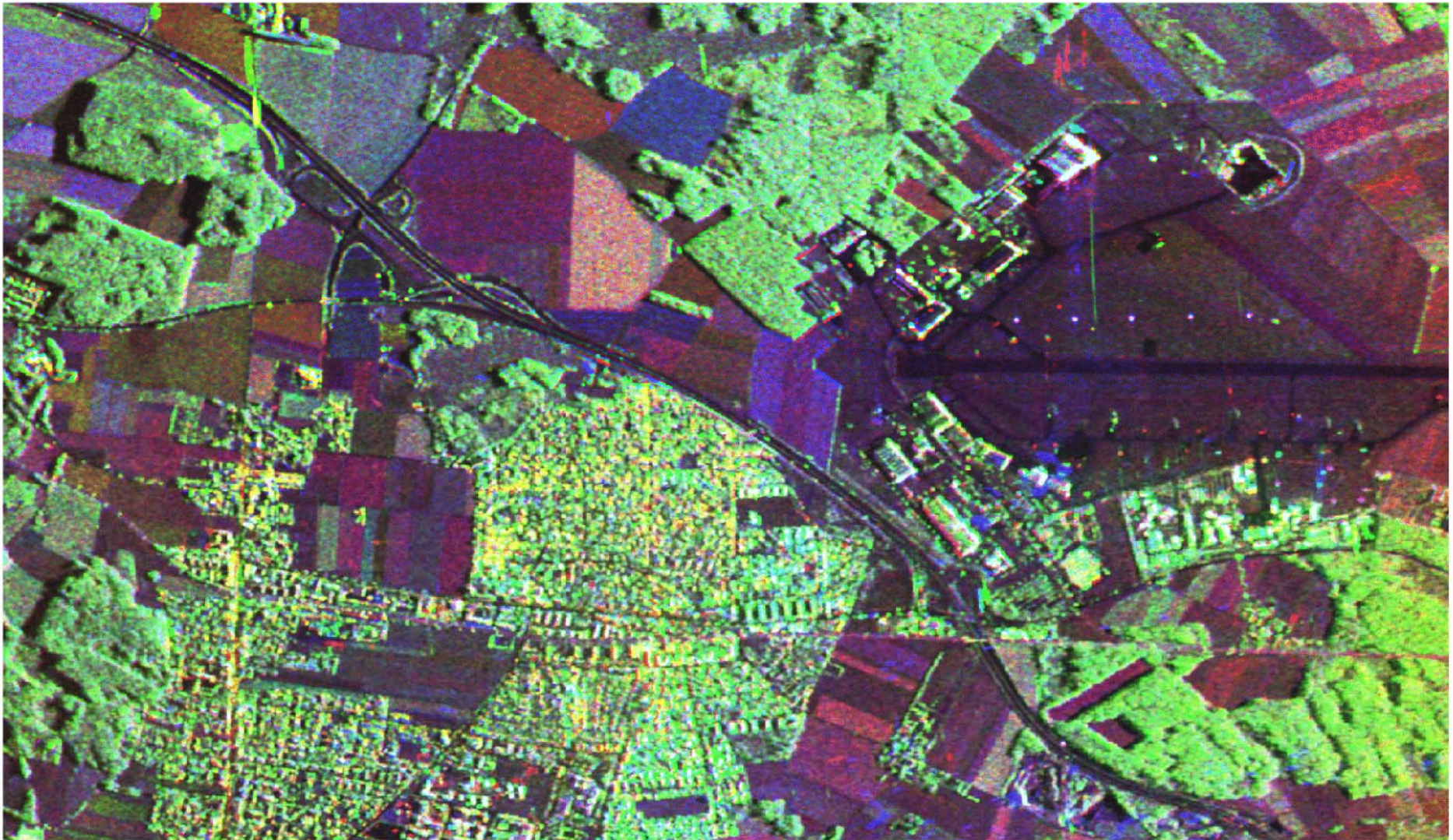
SAR imaging
b






Spotlight image
0.46 m azimuth resolution

1

Multi-Frequency E-SAR-Image (L, C, and X-band)



 L-band, HH  C-band, HH  X-band, VV

Processing Principles

Coherence

If phases φ of waves random & (directly or in effect) uniformly distributed

$0 \leq \varphi \leq 2\pi \rightarrow$ incoherent.

If phase relations between waves are constant \rightarrow coherent

Correlation

$$C = \frac{\langle (E_1(t)E_2^*(t)) \rangle}{\sqrt{\langle E_1(t)E_1^*(t) \rangle \langle E_2(t)E_2^*(t) \rangle}} \quad -1 \leq C \leq +1$$

E_1 and E_2 vary in conformity $\rightarrow C=1$, E_1 and E_2 vary in opposition $\rightarrow C=-1$

Coherence: $\gamma = |C| = \left| \frac{\langle (E_1(t)E_2^*(t)) \rangle}{\sqrt{\langle E_1(t)E_1^*(t) \rangle \langle E_2(t)E_2^*(t) \rangle}} \right| \quad 0 \leq \gamma \leq 1$

$\gamma = 0$ means \rightarrow incoherence, $\gamma = 1 \rightarrow$ complete coherence

Continuous transition from pure coherence to pure incoherence

SAR Processing Basics

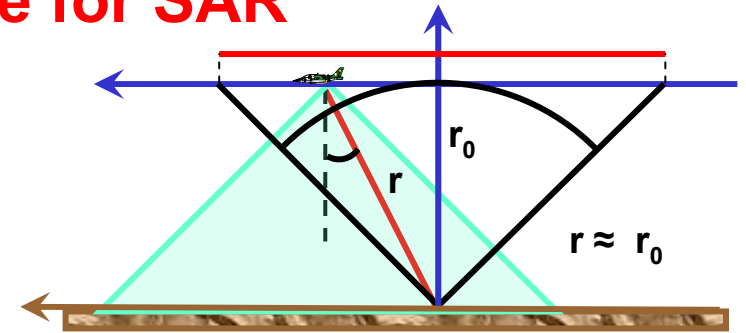
Phase Information is decisive for SAR

$$r^2 = r_0^2 + (vt)^2 \implies (r - r_0) \approx \frac{(vt)^2}{2r_0}$$

$$r \approx r_0 + \frac{(vt)^2}{2r_0}$$

Two Way Phase: $\varphi = \frac{2\pi}{\lambda} \left(r_0 + \frac{v^2 t^2}{2r_0} \right) \implies \omega_D = 2\pi f_D = \frac{d\varphi}{dt} = 4\pi \frac{v^2}{\lambda r_0} t$

x



Transmitted: $V_T = V_1 \sin \omega t \rightarrow$ Received: $V_r = V_2 \sin(\omega t + \omega_D t)$

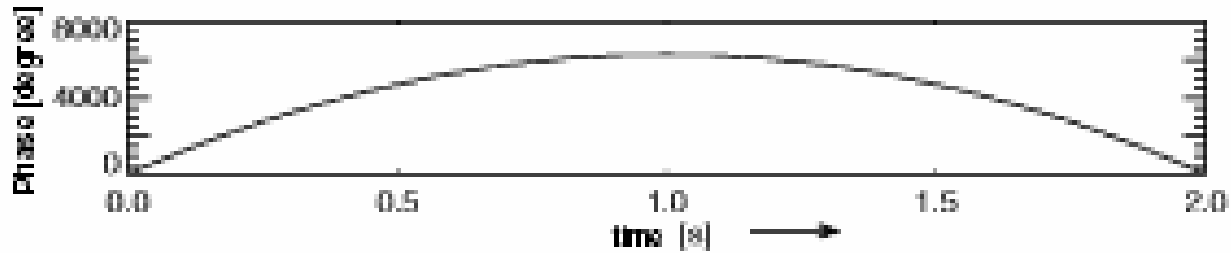
Linear Frequency Modulation

Chirp Steepness: $\frac{2v^2}{\lambda r_0}$

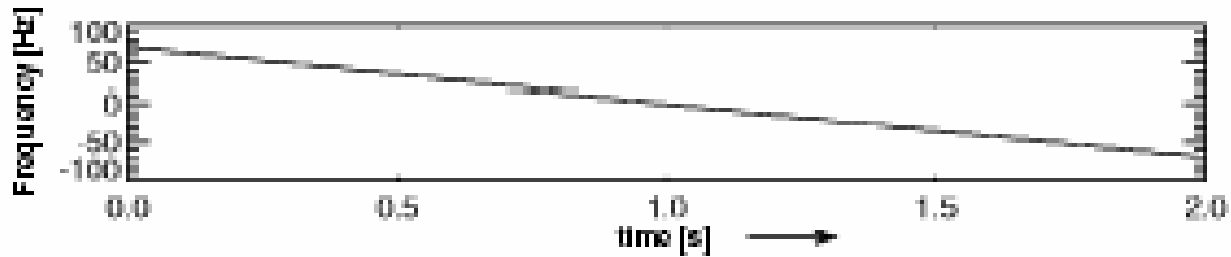
Bandwidth Required: $B_{f_D} = \frac{2v^2}{\lambda r_0} T_D = \frac{2v}{\delta_{az}}$

Azimuth Signal

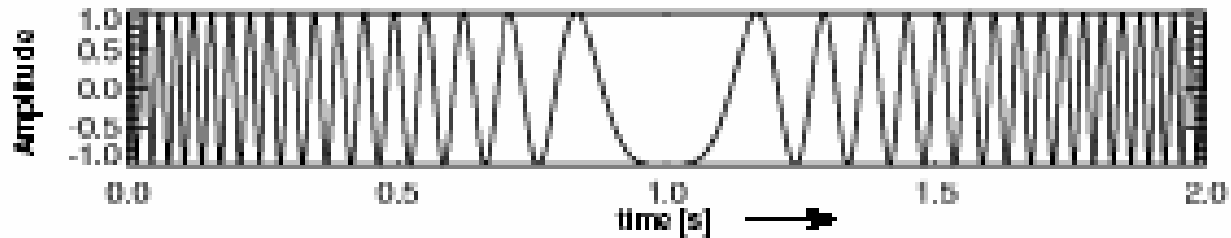
Phase/Degree



Frequency/Hz



Normalized
Amplitude



$$V = 70 \text{ msec}^{-1}, \lambda = 5,6 \text{ cm}, r_o = 5000 \text{ m}$$

Phase Reference

Phase contains all Target Information required. Quadratic Demodulation provides Phase Information with **INPHASE (I) & QUADRATURE (Q)** Component.

$$I(t) = A \cos\left(2\pi \frac{v^2 t}{\lambda r_o} t\right) \quad \& \quad Q(t) = A \sin\left(2\pi \frac{v^2 t}{\lambda r_o} t\right)$$

$$S_{sig}(t) = I(t) + jQ(t) = \exp\left(j2\pi \frac{v^2 t}{\lambda r_o} t\right) \quad \text{with } A = 1$$

Target Position at $t=0$ where $f_D = 0$

Further Information by Correlation with Reference Function for Point Target

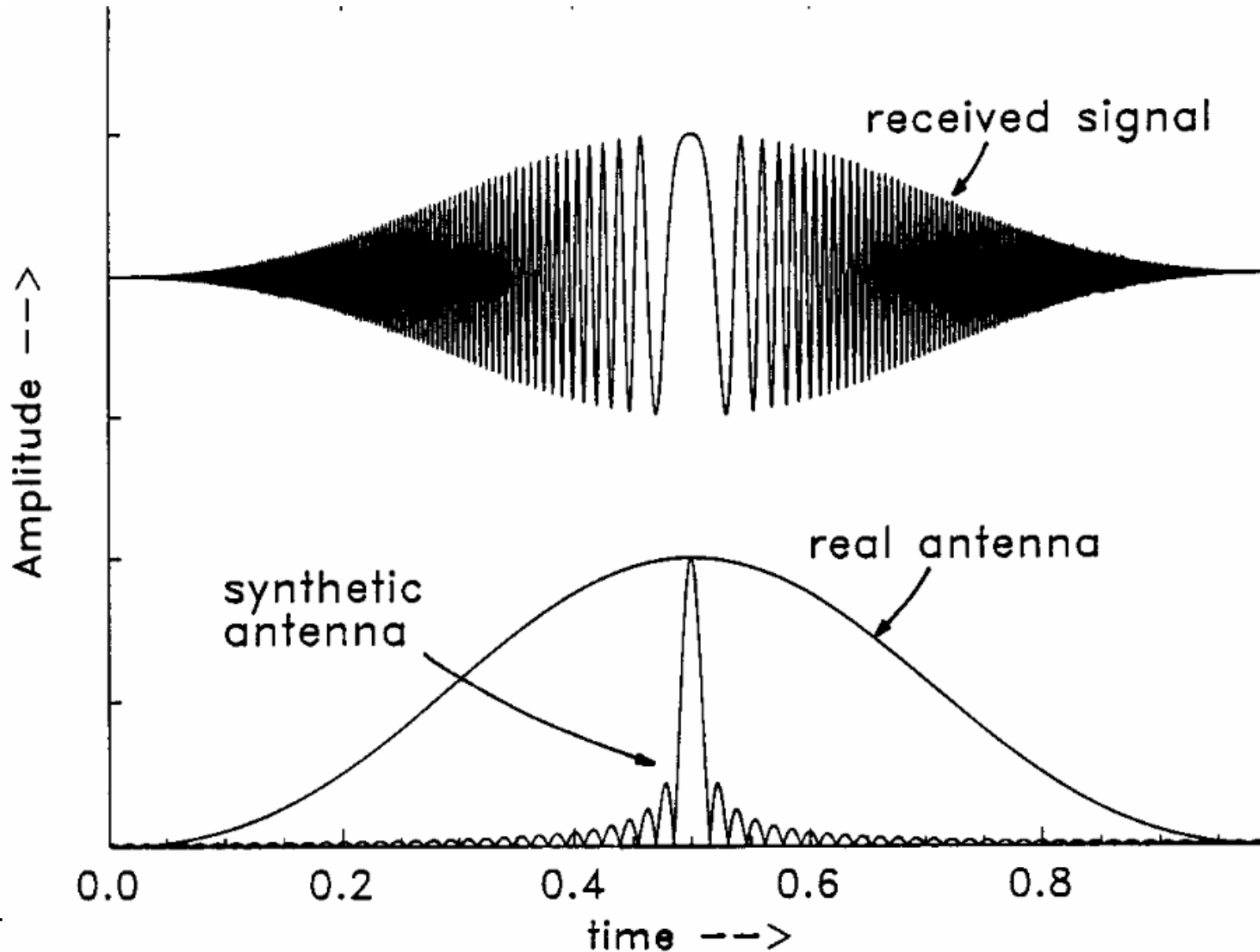
$$S_{ref}(t) = S_{sig}(t)$$

$S_o(t)$ at Correlator Output

$$S_{cor}(t) = \int_{-\frac{T_D}{2}}^{+\frac{T_D}{2}} S_{sig}(t) S_{ref}^*(t - \tau) dt = \exp\left(-j2\pi \frac{v^2 \tau}{\lambda r_o}\right) \int_{-\frac{T_D}{2}}^{+\frac{T_D}{2}} \exp\left(-j2\pi \frac{v^2 \tau}{\lambda r_o} t\right) dt$$

$$S_{cor}(\tau) = \exp\left(-j2\pi \frac{v^2 \tau^2}{\lambda r_o}\right) \text{sinc}\left(\pi \frac{v^2 T_D}{\lambda r_o} \tau\right)$$

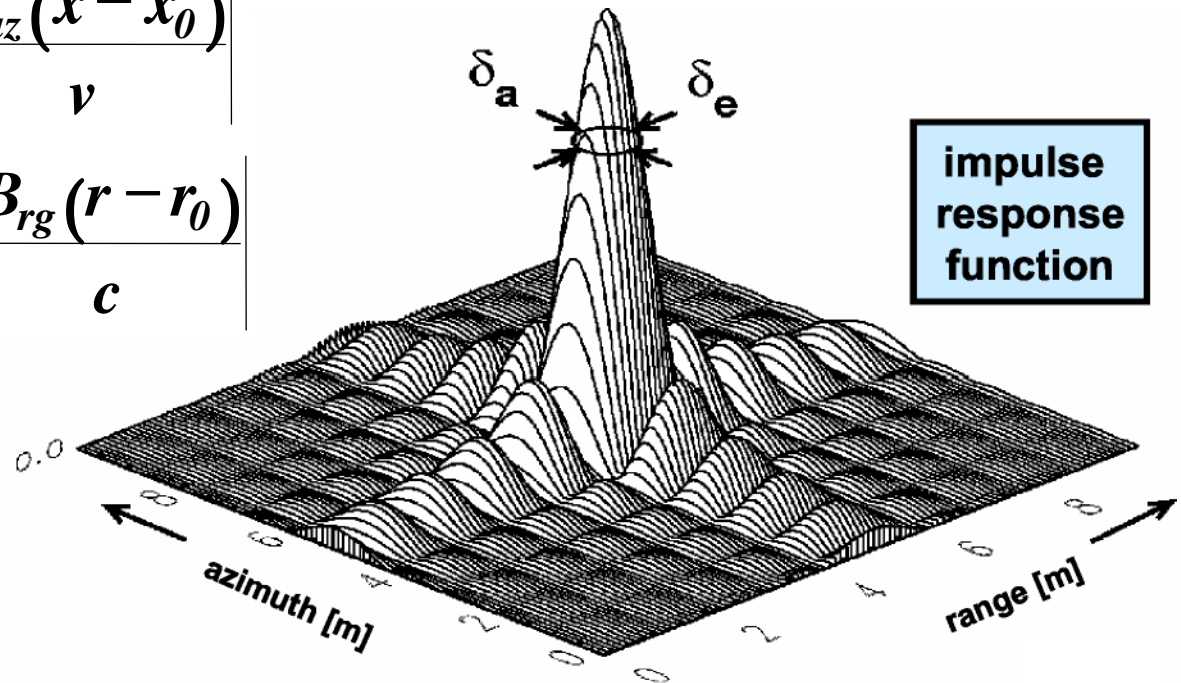
RAR – SAR Point Target Signal Comparision



SAR Processing uses Pulse Response Function in both Azimuth and Range Impulse Response Function

$$|s_{az}(x)| = \left| \sqrt{B_{az} T_D} \operatorname{sinc} \left| \pi \frac{B_{az}(x - x_0)}{v} \right| \right|$$

$$|s_{rg}(r)| = \left| \sqrt{B_{rg} T_{rg}} \operatorname{sinc} \left| 2\pi \frac{B_{rg}(r - r_0)}{c} \right| \right|$$

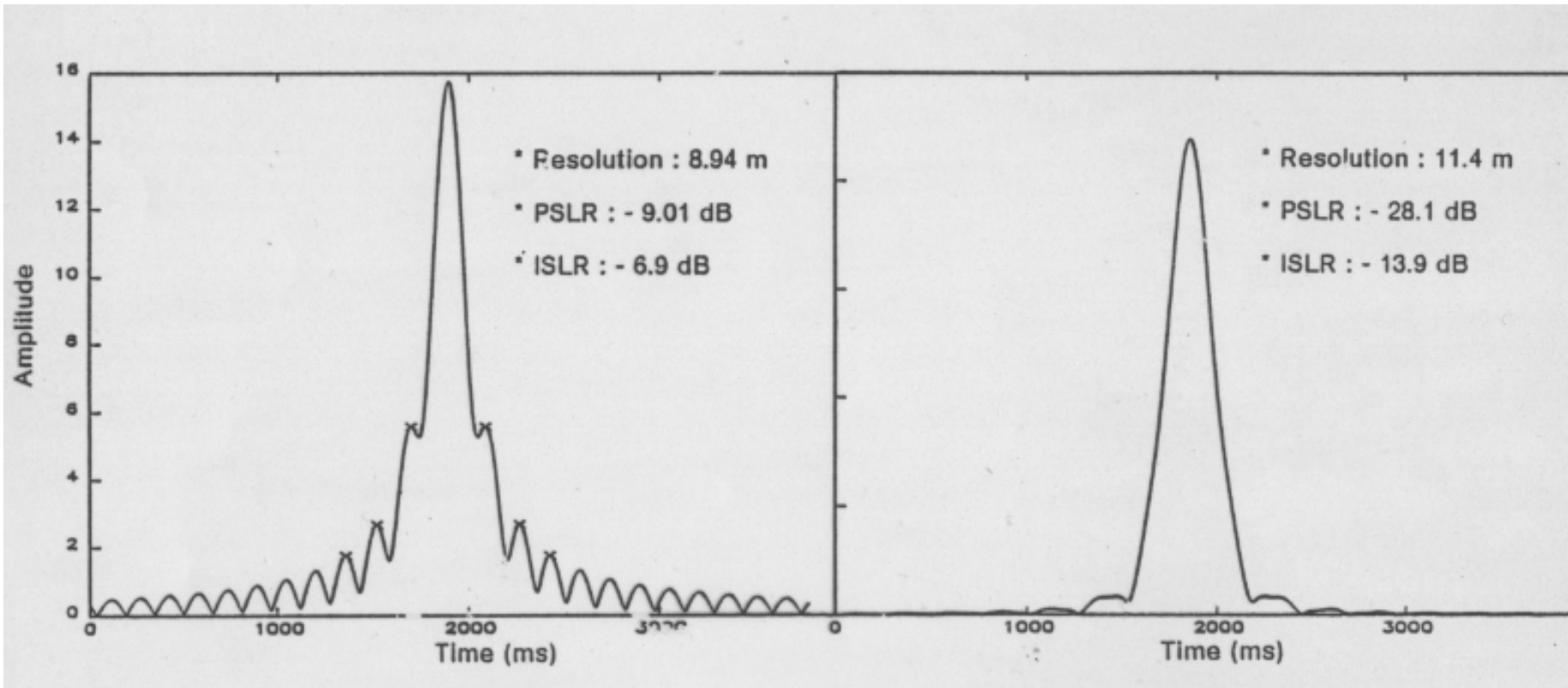


Quality Measures

Peak Sidelobe Ratio & Integrated Sidelobe Ratio

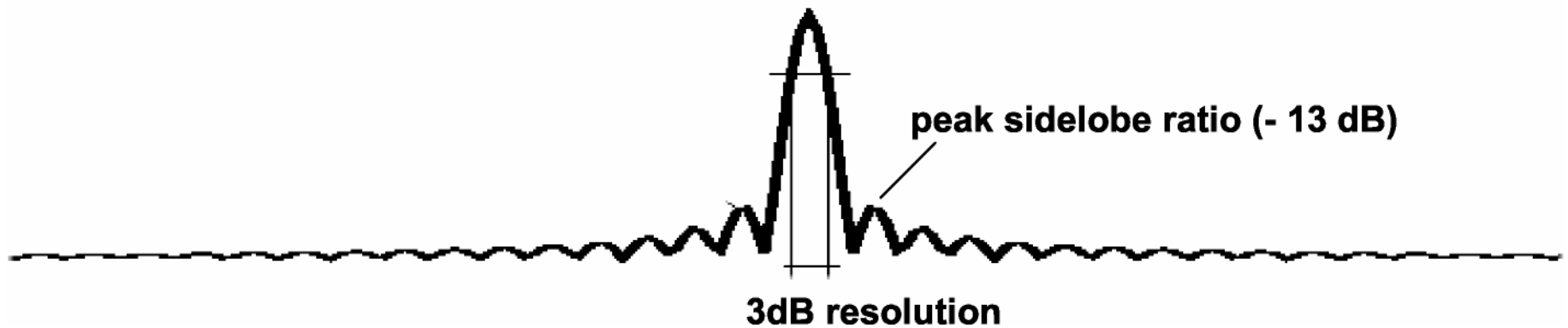
$$\text{PSLR} = \frac{\text{Power within Sidelobes}}{\text{Power within Main Beam}}$$

$$\text{ISLR} = \frac{\text{Power within Sidelobes}}{\text{Power within Diagram}}$$

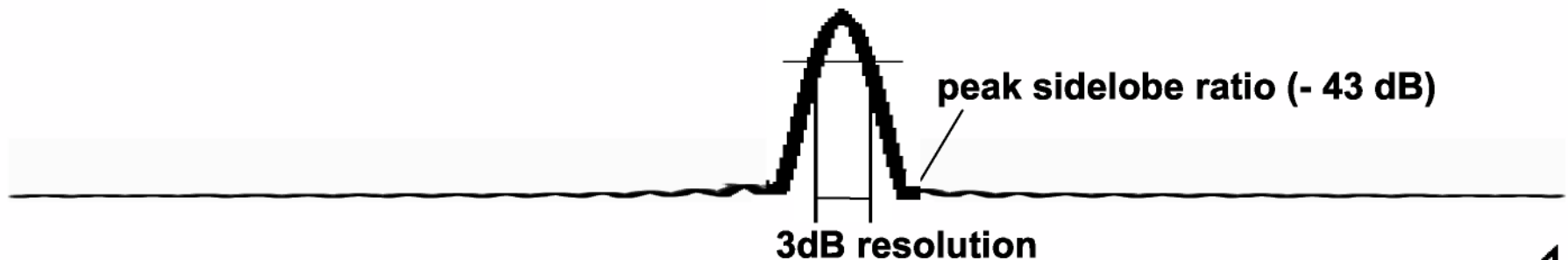
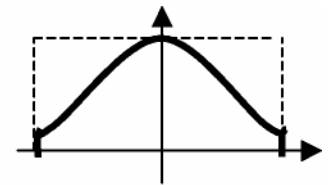


Influence of Weighting

- Impulse response function without weighting: $\text{sinc}(x) = \sin(x)/x$



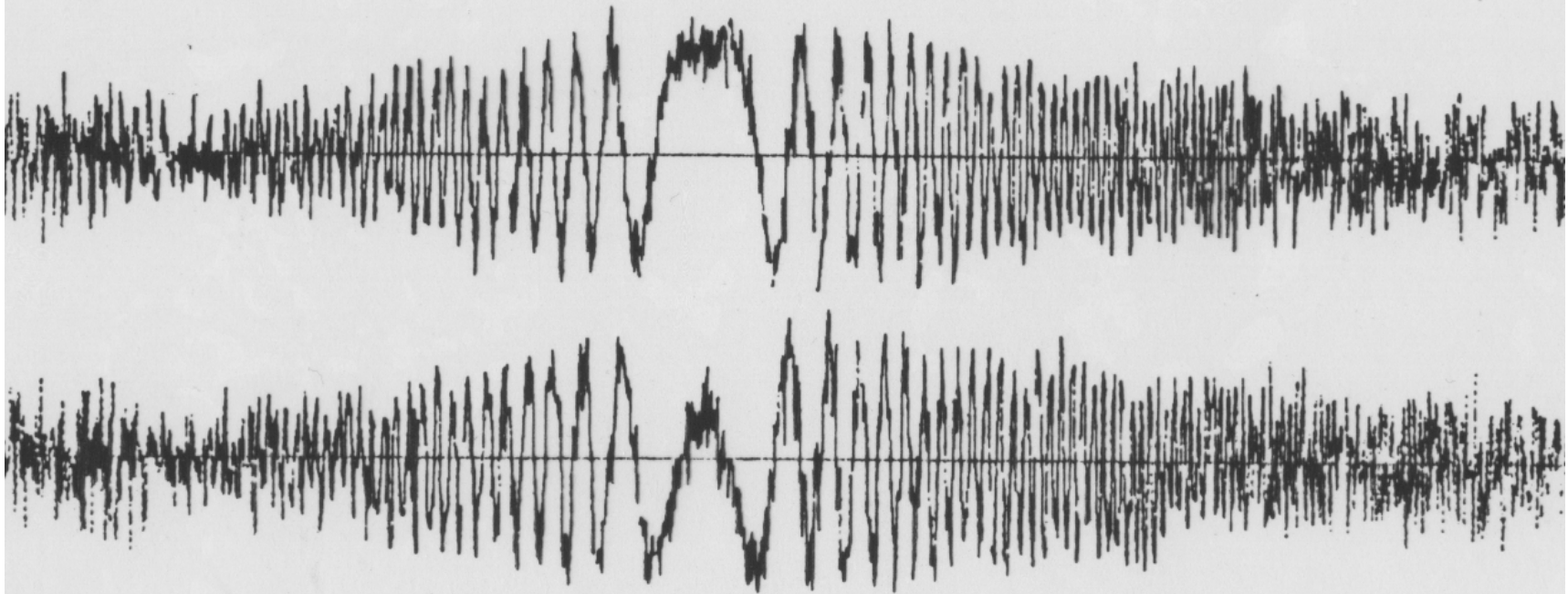
Impulse response function with Hamming weighting ($= 0.54$) $w(t) =$



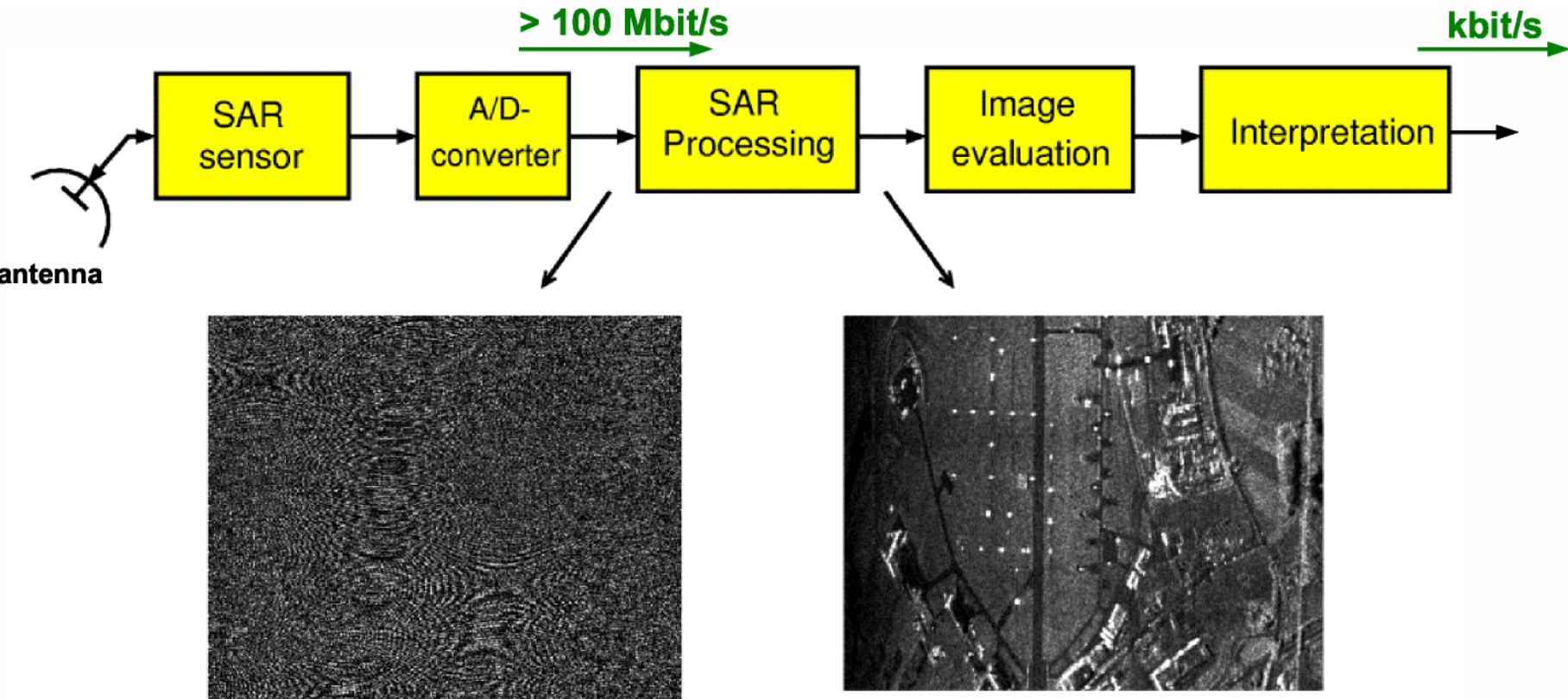
SAR, Measured I- & Q-Signals

Point Target, Frequency Modulated Signals

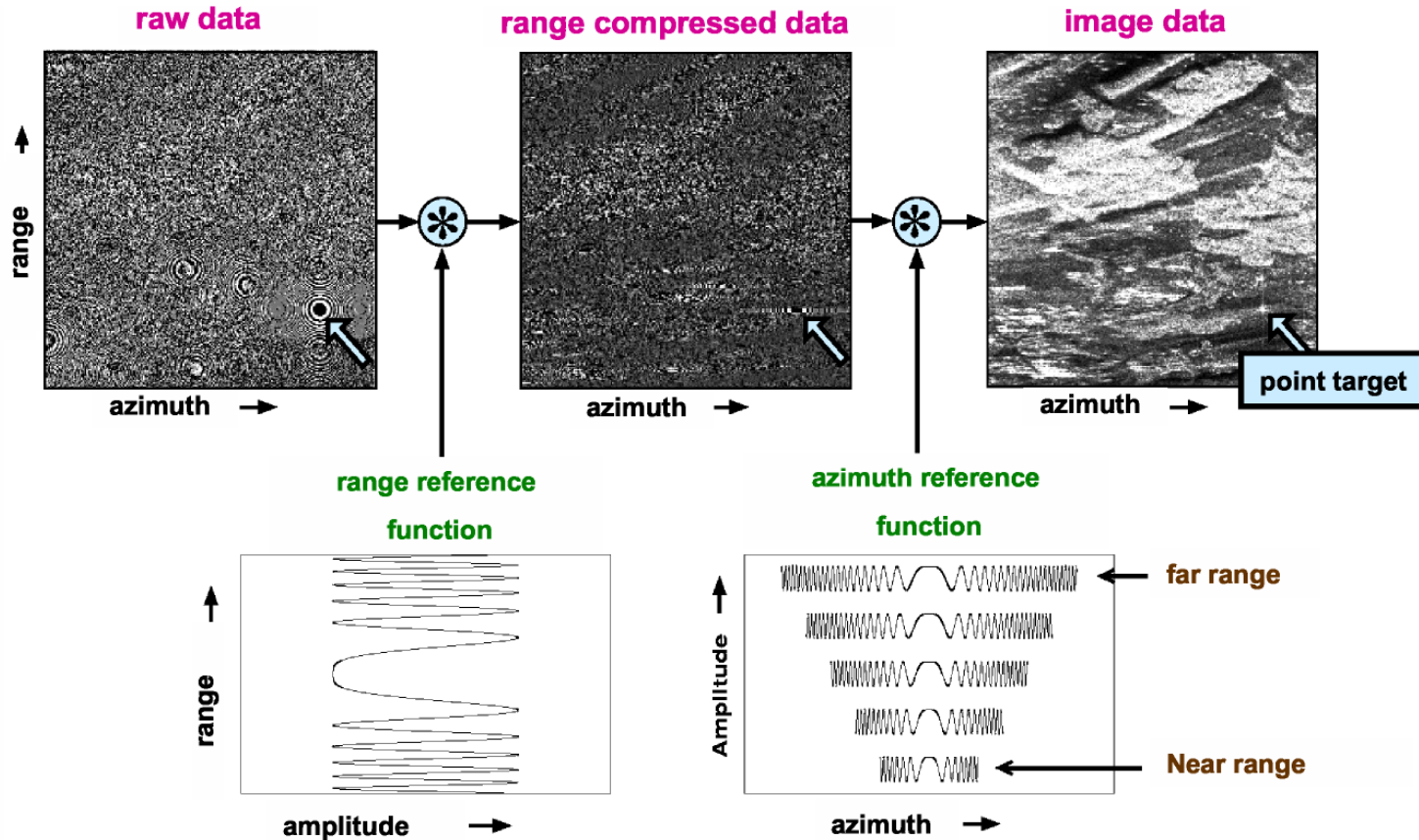
L-Band, $H = 400\text{m}$, $r_0 = 1590\text{m}$, $v = 60\text{m sec}^{-1}$



SAR Data Flow



SAR Processing Image Formation



Different Azimuth Reference Functions for different Range Gates

Characteristics of Impuls Response Function

Hamming weighting (α)	resolution deterioration factor	PSLR (Peak Sidelobe Ratio)	ISLR (integrated sidelobe ratio)
none	0.88	13.2 dB	9.8 dB
0.54	1.30	43 dB	21 dB

- azimuth resolution

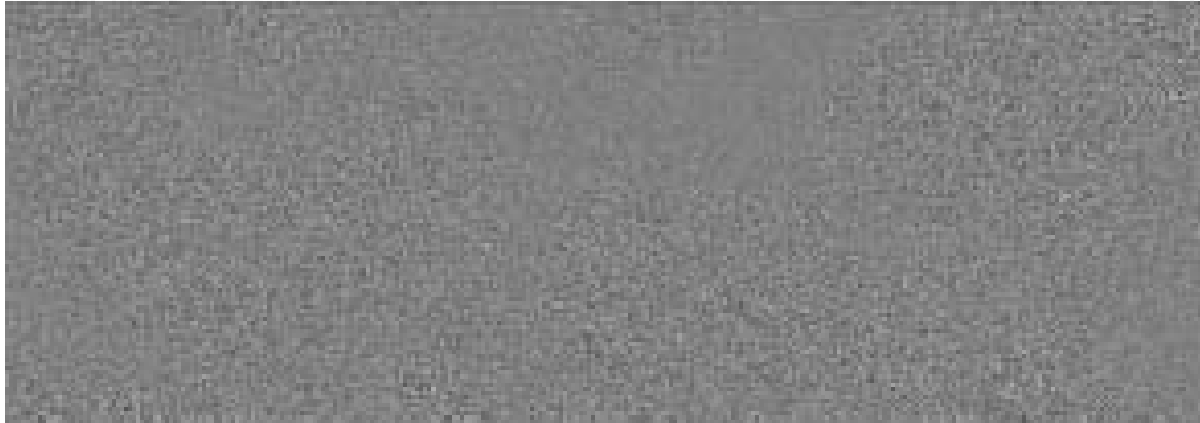
$$\delta_a = k_a \cdot \frac{v}{B_a} = k_a \cdot \frac{d_a}{2}$$

k_a = azimuth resolution deterioration factor

- range resolution

$$\delta_e = k_e \cdot \frac{c_0}{2 \cdot B_e}$$

k_e = range resolution deterioration factor

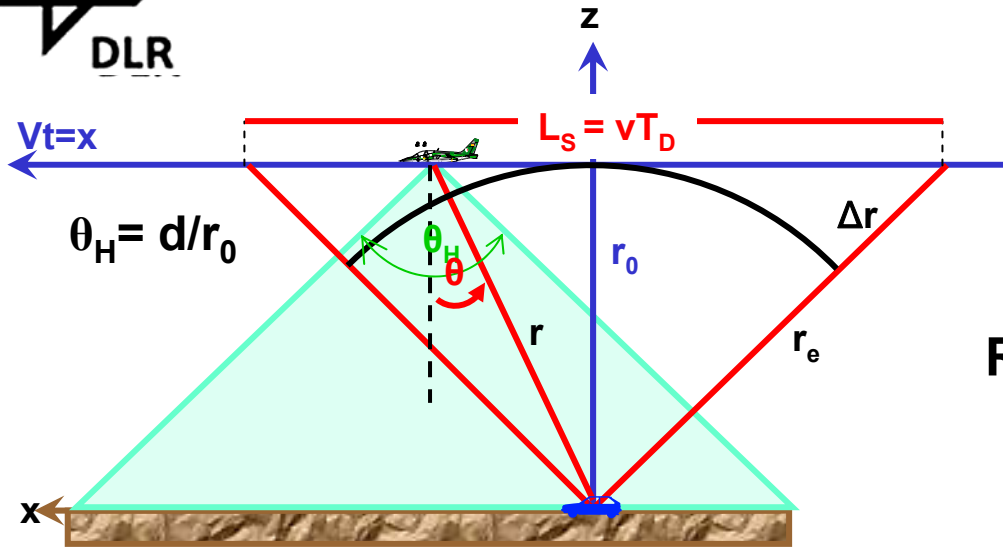


Raw Data



SAR Image

Unfocussed SAR



Focussed SAR needs Phase Compensation during Dwell Time
Unfocussed SAR ignores $\Delta r \leq \lambda/16$

Required Dwell Time for Specified δ_{az}

$$T_D = \frac{\lambda r}{v \delta_{az}}$$

$$(L_s/2)^2 = r_o^2 - r_e^2 \approx 2r_o(r_e - r_o)$$

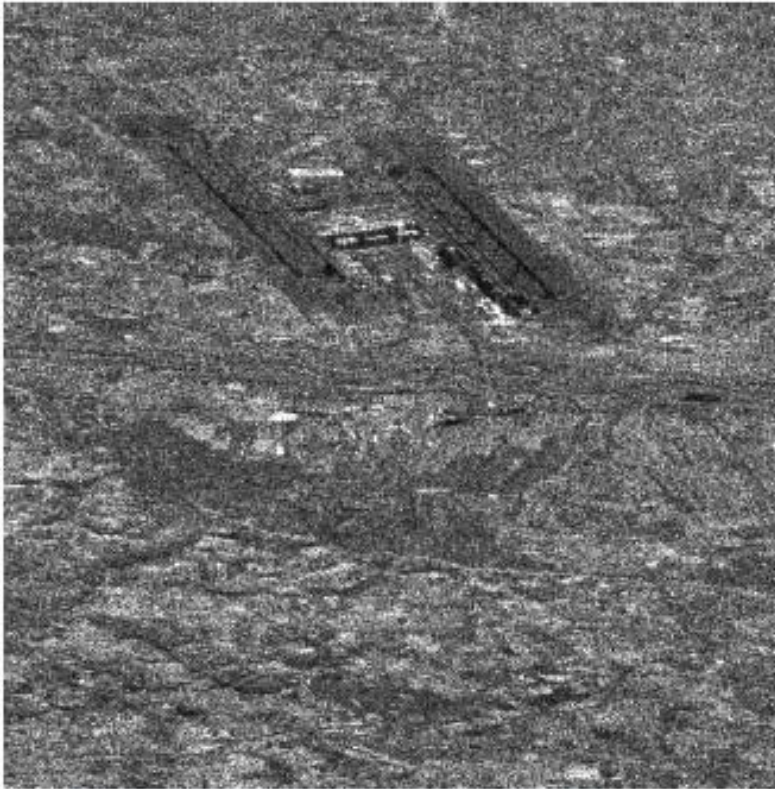
$\Delta r \leq \lambda/16 \Rightarrow$ Maximum Apertur Length for Unfocussed SAR

$$L_{Sunmax} \leq \sqrt{\frac{r_o d}{2}}$$

Resolution obtainable for Unfocussed SAR

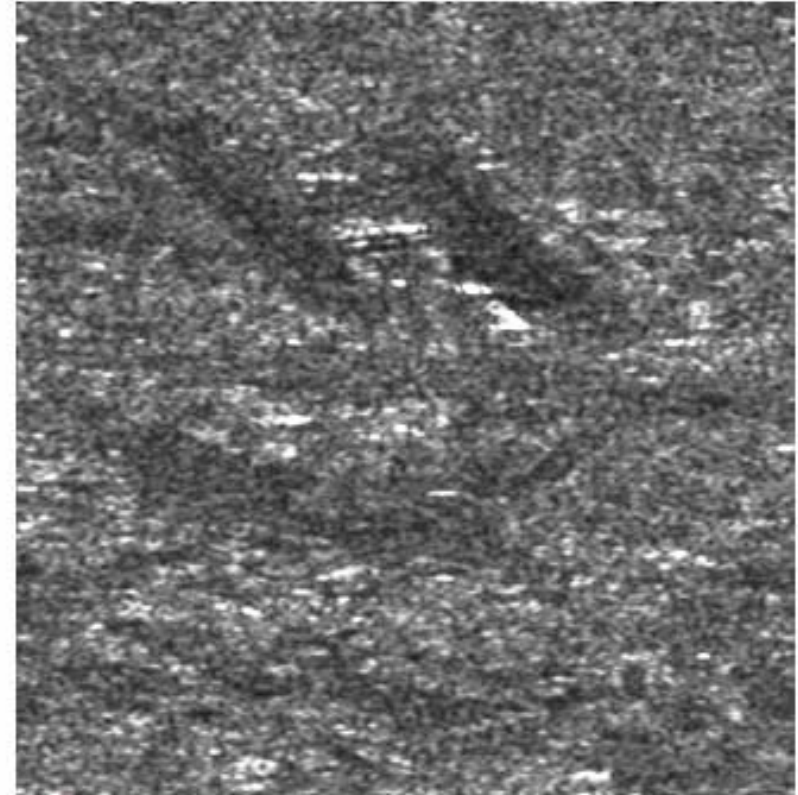
$$\delta_{azunfoc} = \frac{1}{2} \sqrt{r \lambda}$$

Focussed vs. Unfocussed Processing, Munich Airport ERS-1



Focused Processing

- one azimuth look,
- one range look
- 7 m Azimuth resolution,
- 9 m range resolution

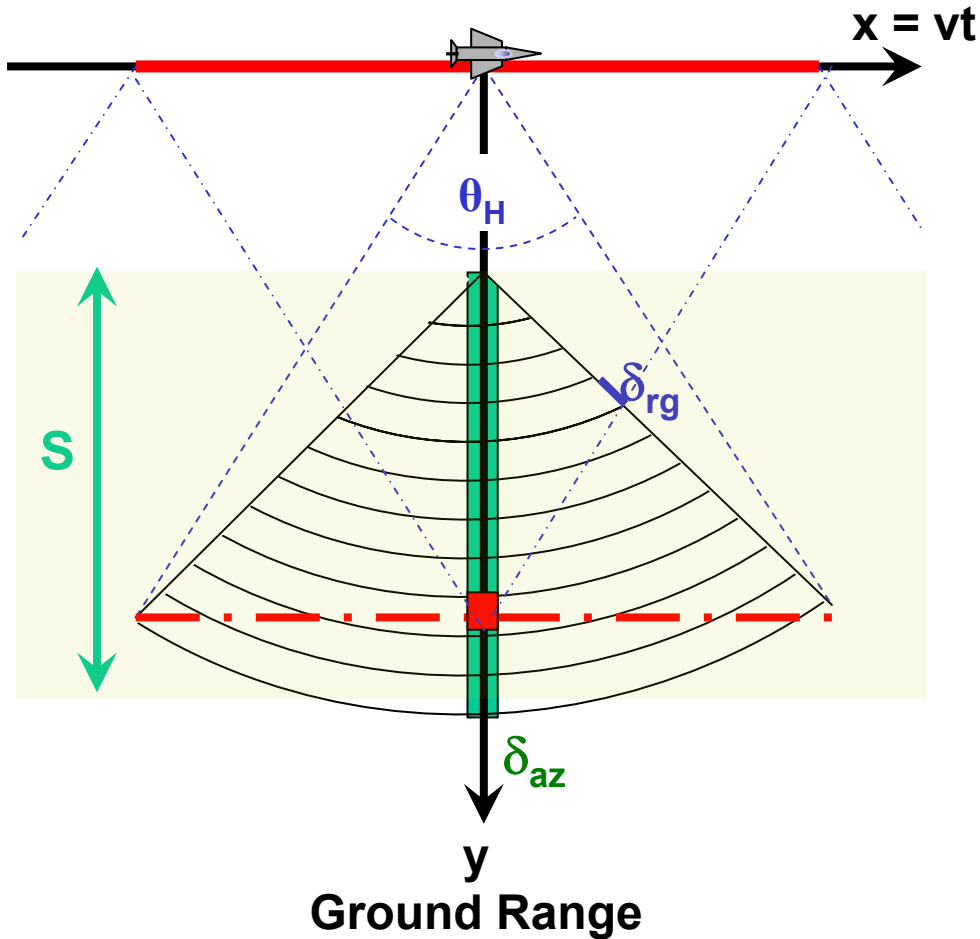


Unfocused Processing

- unfocussed azimuth processing
- 4 range looks
- 110 m azimuth
- 36 m range resolution

Depth of Focus (DOF)

Defines Nr. of Reference Functions required over the Whole Swath



Definition

$$\text{DoF} = 2\Delta r_0$$

Required **Accuracy** to match a given quadratic Phase Reference Function to the considered Range
Maximum allowed Phase Error

$$|\Delta r - \Delta r_0| = \lambda/8$$

Depth of Focus (DOF)

Defines Nr. of Reference Functions required over the Whole Swath

Definition: DoF = $2\Delta r_0$

Required **Accuracy** to match a given quadratic Phase Reference Function to the considered Range for Maximum allowed Phase Error **$|\Delta r - \Delta r_0| = \lambda/8$**

$$r^2 = r_0^2 + \left(\frac{L_s}{2}\right)^2 \rightarrow \frac{dr}{dr_0} = 2r \frac{dr}{dr_0} = 2r_0 \rightarrow \frac{\Delta r}{\Delta r_0} = \frac{r_0}{\sqrt{r_0^2 + \left(\frac{L_s}{2}\right)^2}} \approx 1 - \frac{1}{8} \frac{L^2}{r_0^2}$$

$$|\Delta r - \Delta r_0| = \Delta r_0 \frac{L^2}{2(2r_0)^2} = \frac{\lambda}{8}$$

$$\boxed{DOF = 2\Delta r_0 = 2\lambda \frac{r_0^2}{L^2} = 8 \frac{\delta_{az}^2}{\lambda}}$$

Depth of Focus (2):

$$DOF = 8 \frac{\delta_{az}^2}{\lambda}$$

The depth of focus becomes smaller as δ_{az} is made smaller.

Example:

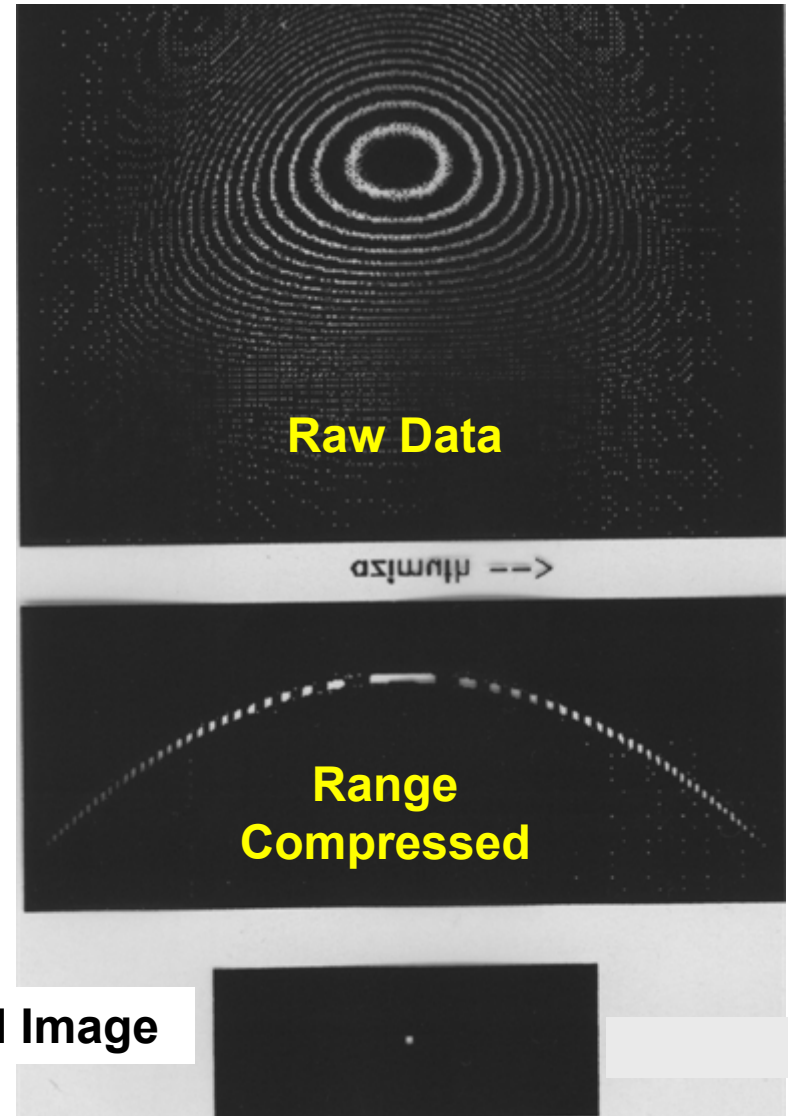
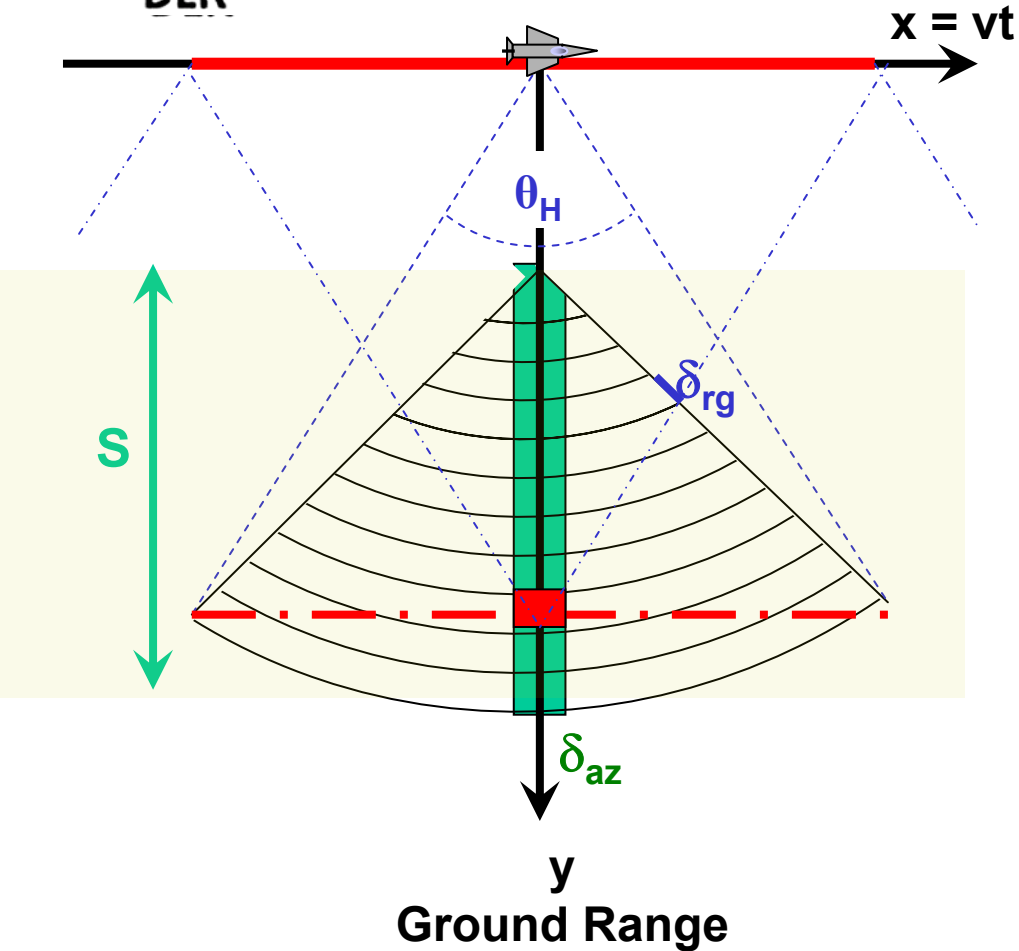
$$X = 5 \text{ cm}, \delta_{az} = 3 \text{ m} \text{ DOF} \approx 1.44 \text{ km}$$

Processing of a 4.3 km swath requires 3 different reference functions.

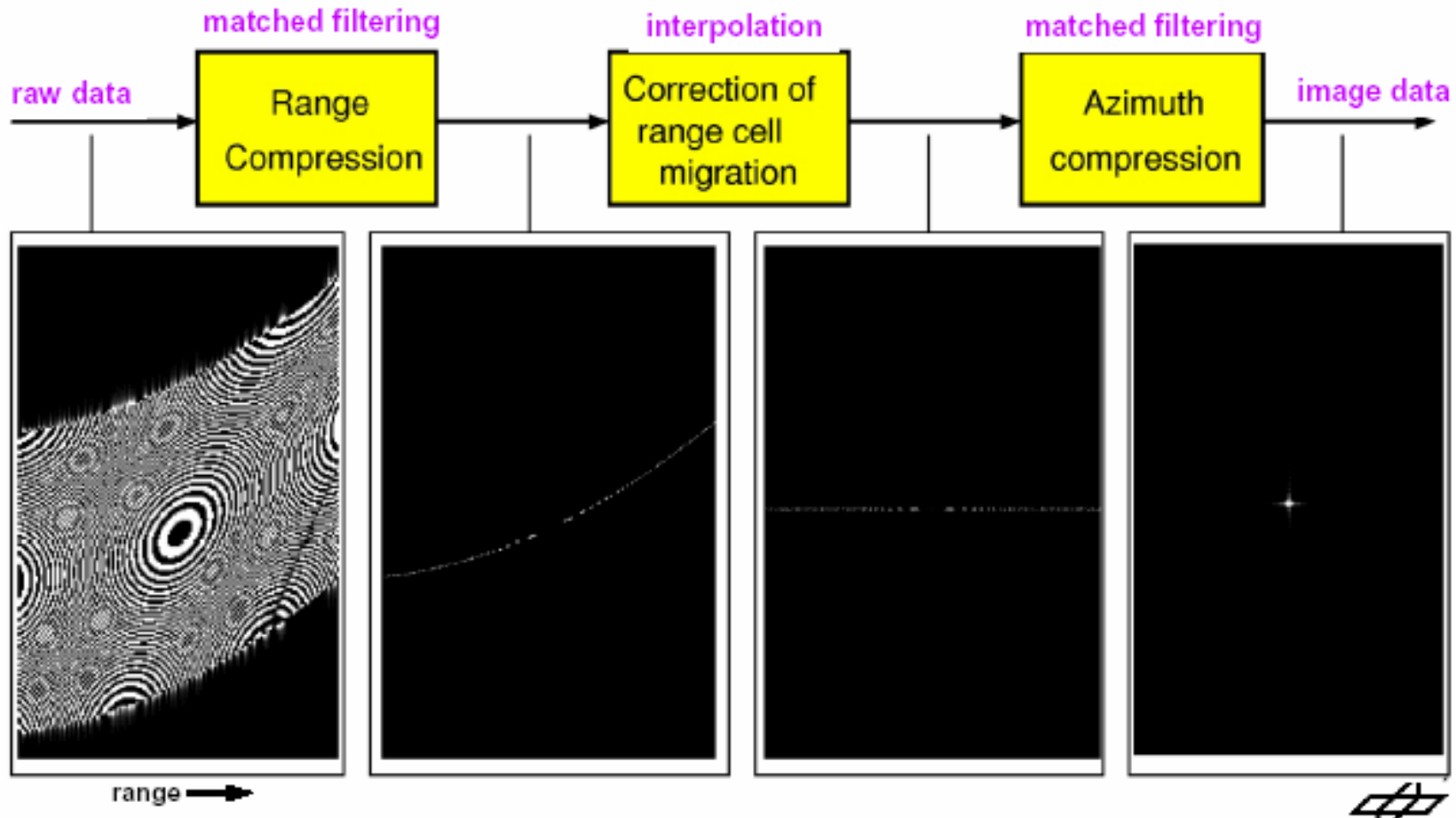
If $\delta_{az} = 50 \text{ cm}$ under the same conditions: $\text{DOF} \approx 40 \text{ m}$

10 references are required increasing the processing complexity.

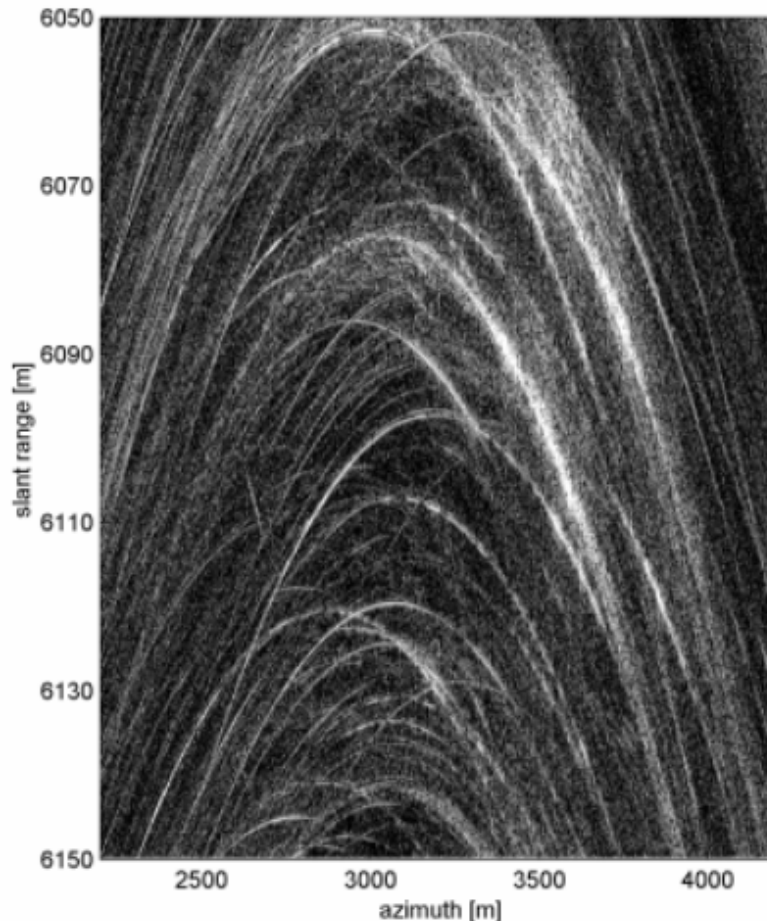
Range Curvature due to Range Cell Migration (2)



SAR Image Formation



Range Curvature Example



Cut out of PAMIR data after range compression, urban area, sliding mode. The processing algorithm has to deal with a distinct range curvature stretching across hundreds of range cells.

[Courtesy FGAN, Ender, Brenner, PAMIR Article, IEE Special Issue EUSAR 2002]

[Ender, Brenner, PAMIR Artikel IEE Special Issue EUSAR 2002,
Courtesy FGAN]

Phase Errors

The Targets Phase History must be Known Precisely

Thump Rule: Phase Jitter may not exceed $\pi/8$ rad of RF-Cycle

Phase Error Reasons

- Radar Platform Instabilities
- Flight Path Deviations
- Target Motion and Acceleration
- Instabilities of SAR-Electronic
- Propagation Path Anomalies
- Orbit Excentricities
- Earth Rotation Effects

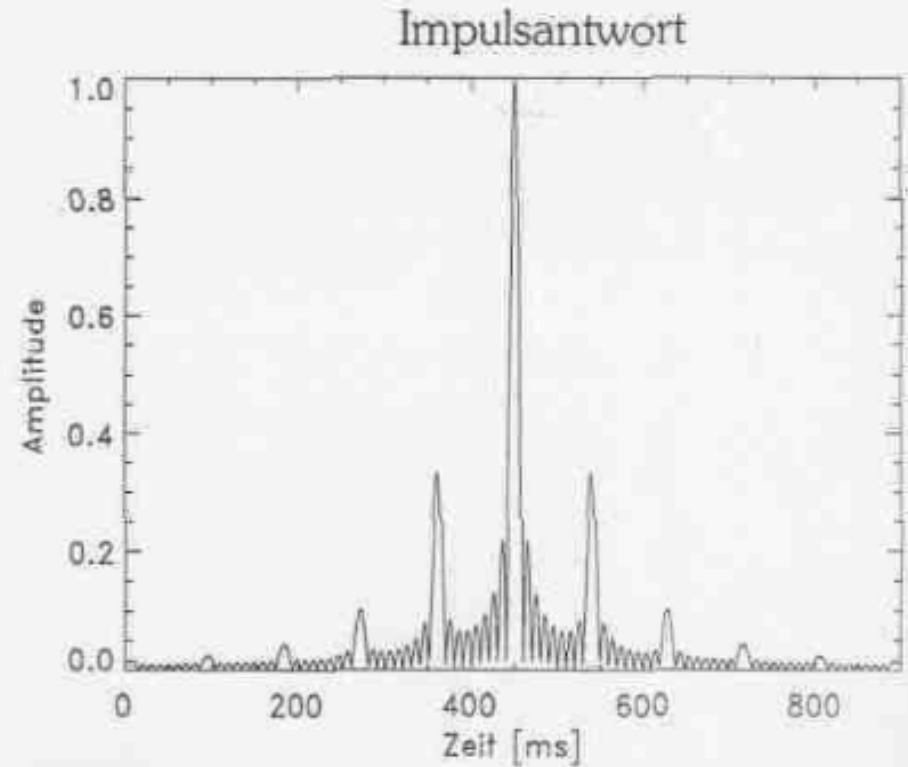
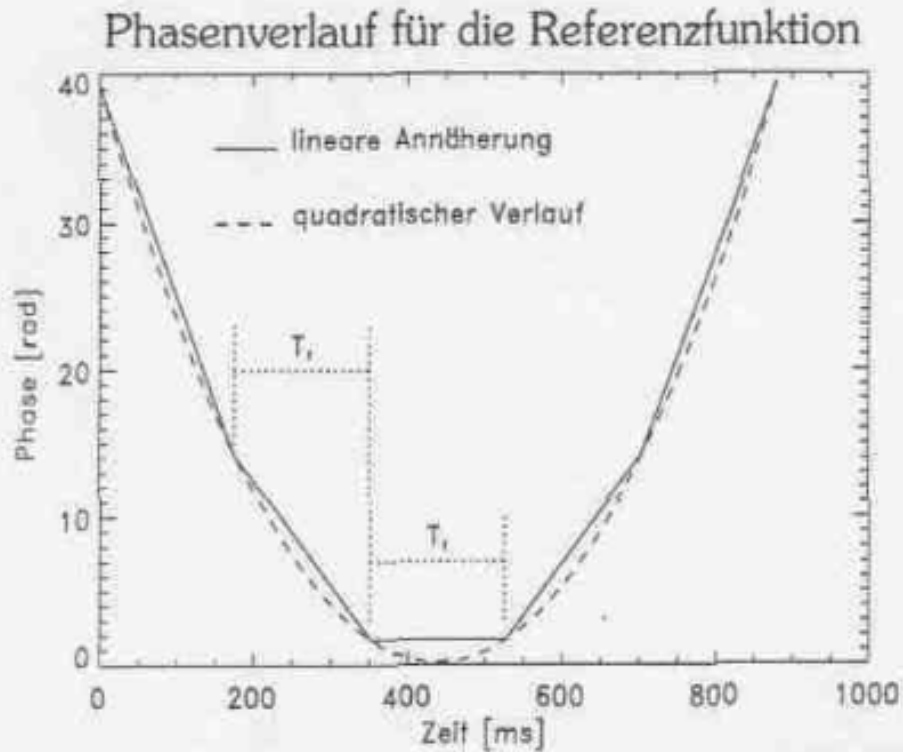
Phase Error Effects

- Decrease in Image Quality
- Range and Azimuth Defocussing
- Loss in Mainlobe Response
- Image Side Lobe Level Increase
- Target Position Shift
- Image Shift
- *Decorrelation*

SAR-Verarbeitung

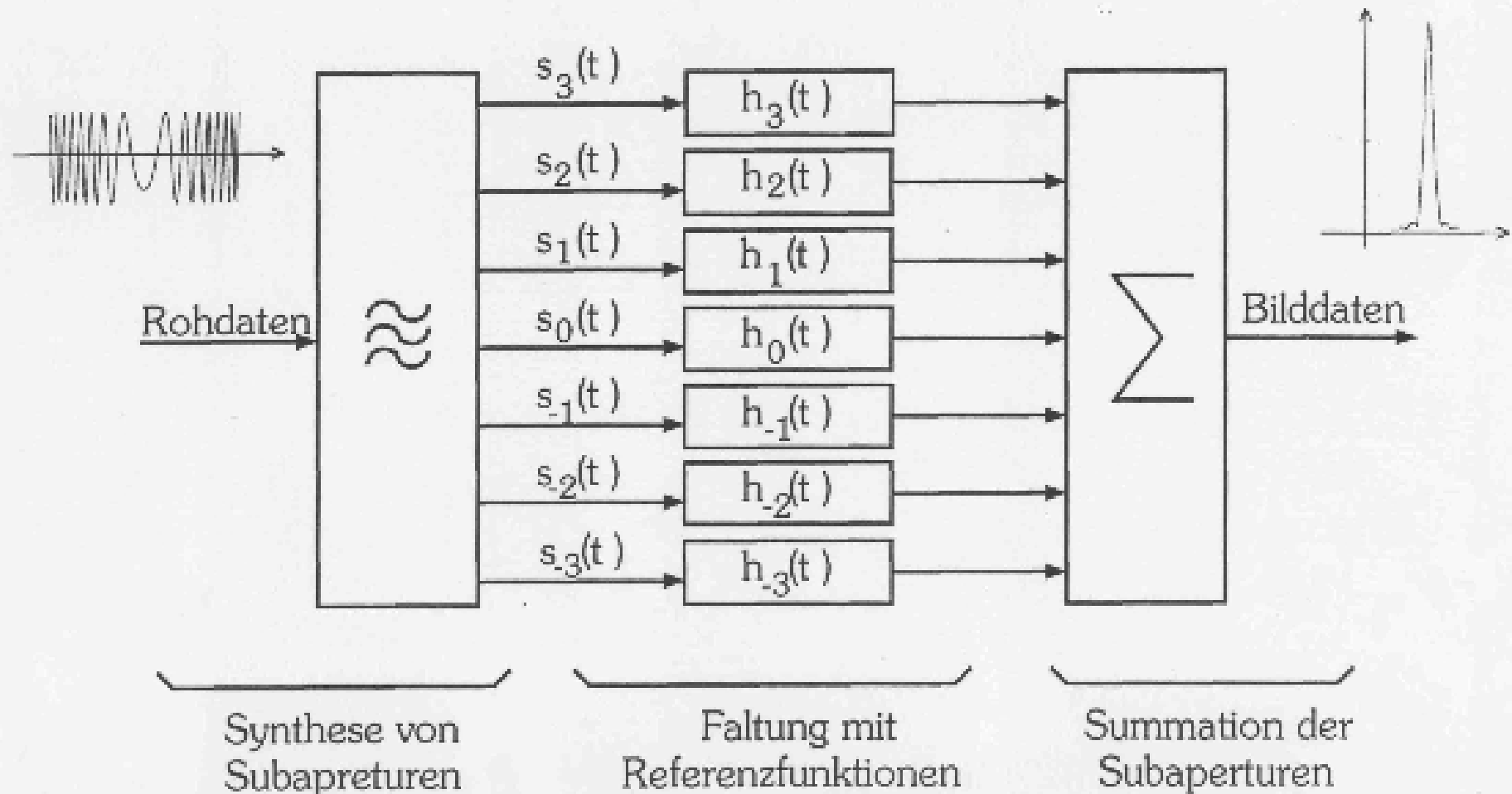
- Eingangsdatenrate: 30 - 100 Mbit/Sekunde
- Geringe Datenreduktion für Rohdaten möglich
- Berechnungsaufwand: $> 5 \times 10^9$ Operationen/Sekunde
- Vorteile der Echtzeit-SAR-Verarbeitung
 - Gesamte SAR-Hardware kann in Echtzeit überprüft werden
 - Echtzeit-Auswertung wird ermöglicht
 - Datenrate kann stark reduziert werden
 - Datenaufzeichnung und Datenübertragung zur Empfangsstation werden vereinfacht
 - Bildprodukte können als Referenz für die Bodenprozessierung benutzt werden
- Welches Verfahren eignet sich für die Echtzeit-SAR-Verarbeitung ?

Näherung für den Phasenverlauf



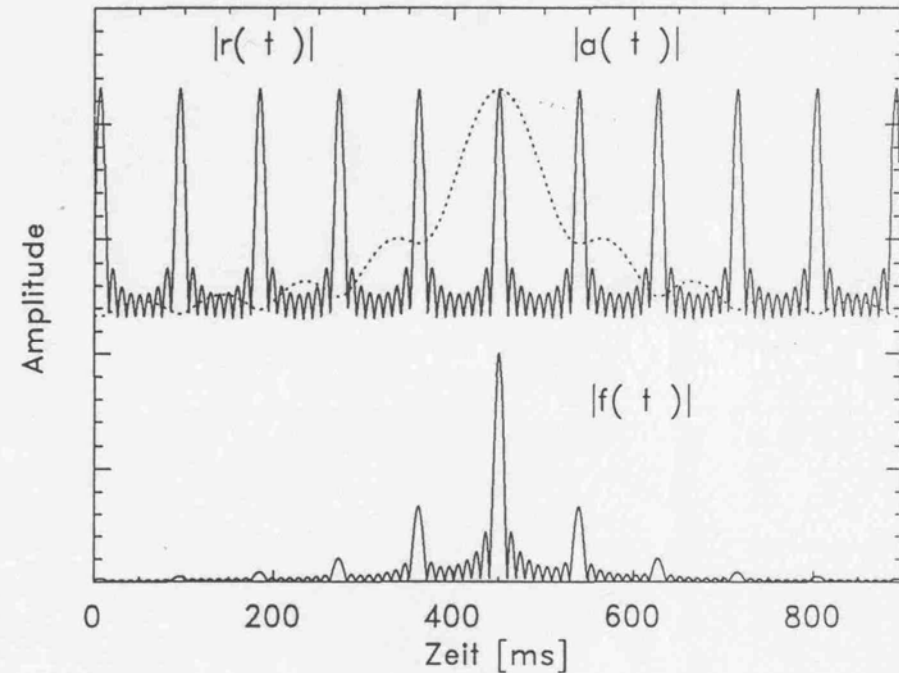
Subaperturverarbeitung

Subaperturprinzip



Analyse der Impulsantwort

- $|f(t)| = \left| \sum_{-N/2}^{N/2} s_n \otimes h_n \right|$
- $|f(t)| = |a(t)| \cdot |r(t)|$

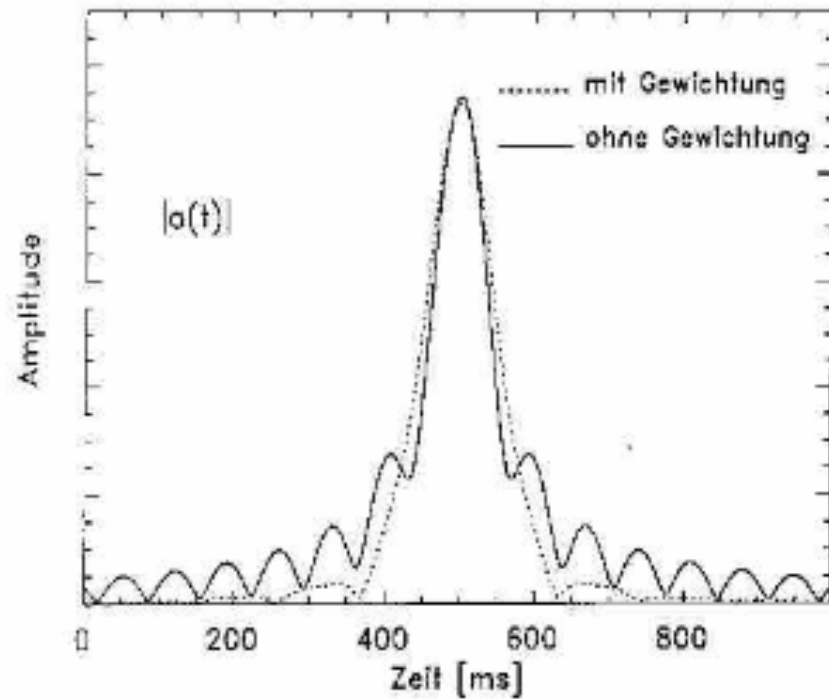


- Impulsantwort $a(t)$ jeder Subapertur entspricht dem Ergebnis der unfokussierten Verarbeitung
- Anforderung an die Bildqualität: Nebenzipfelabstand > 30 dB

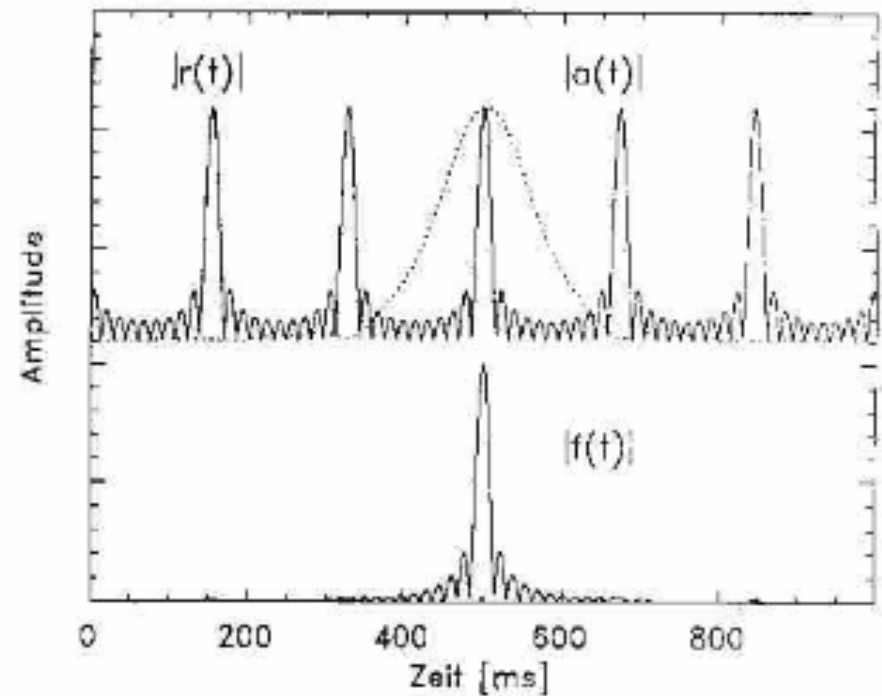


Optimierung der Impulsantwort

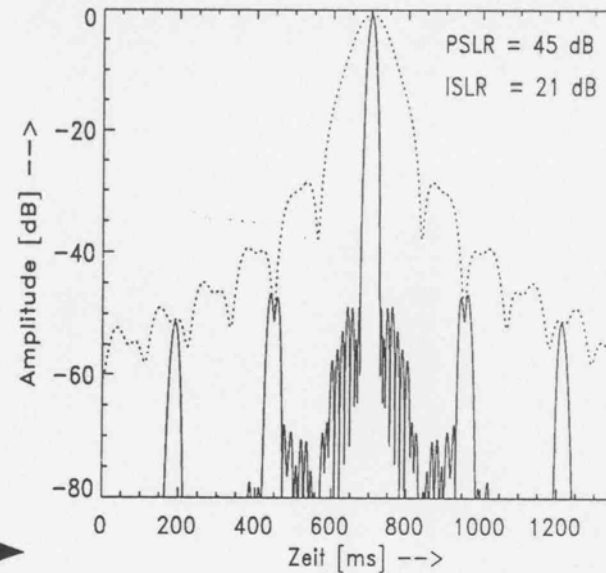
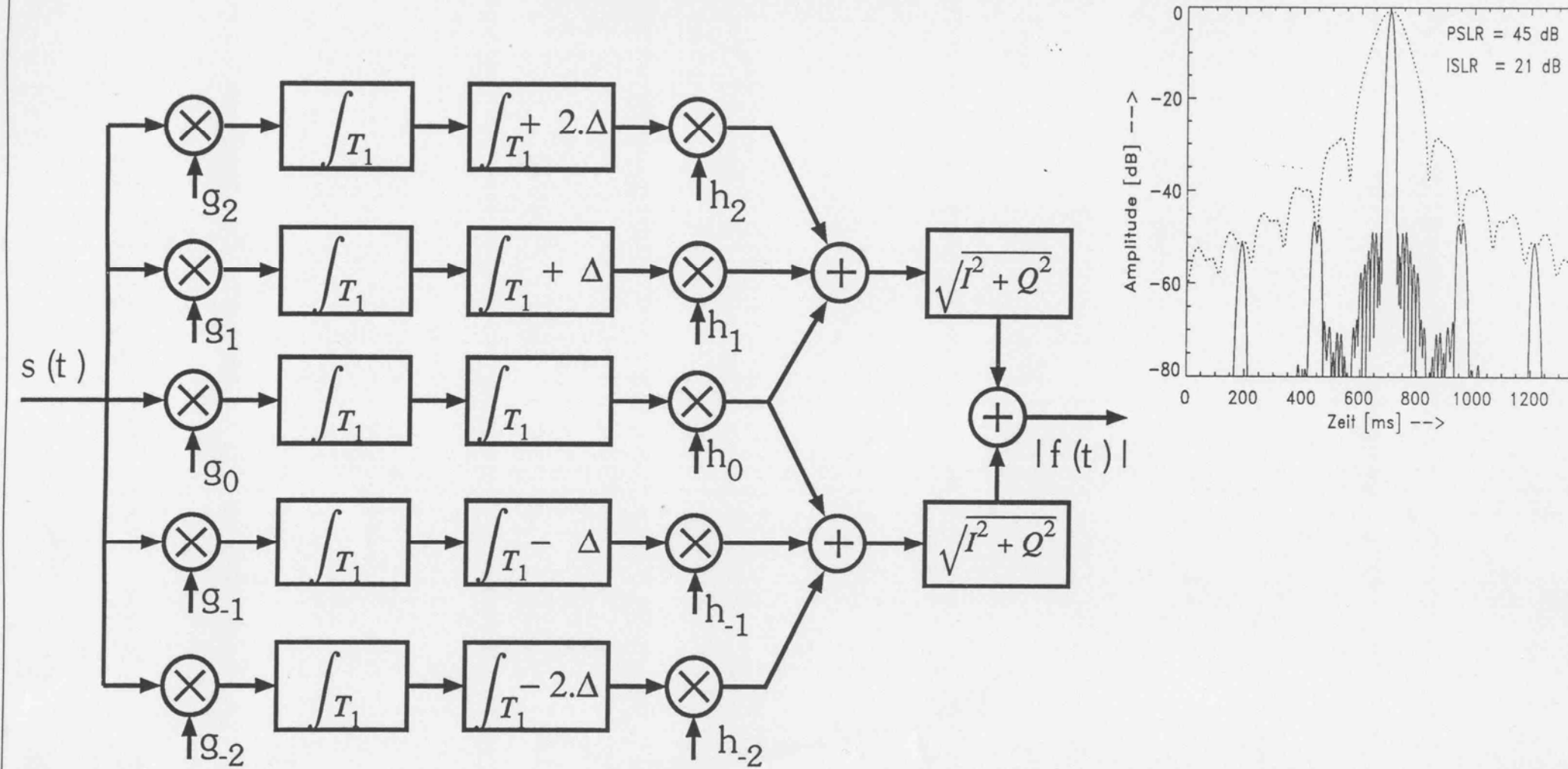
- Einfügung einer Gewichtung



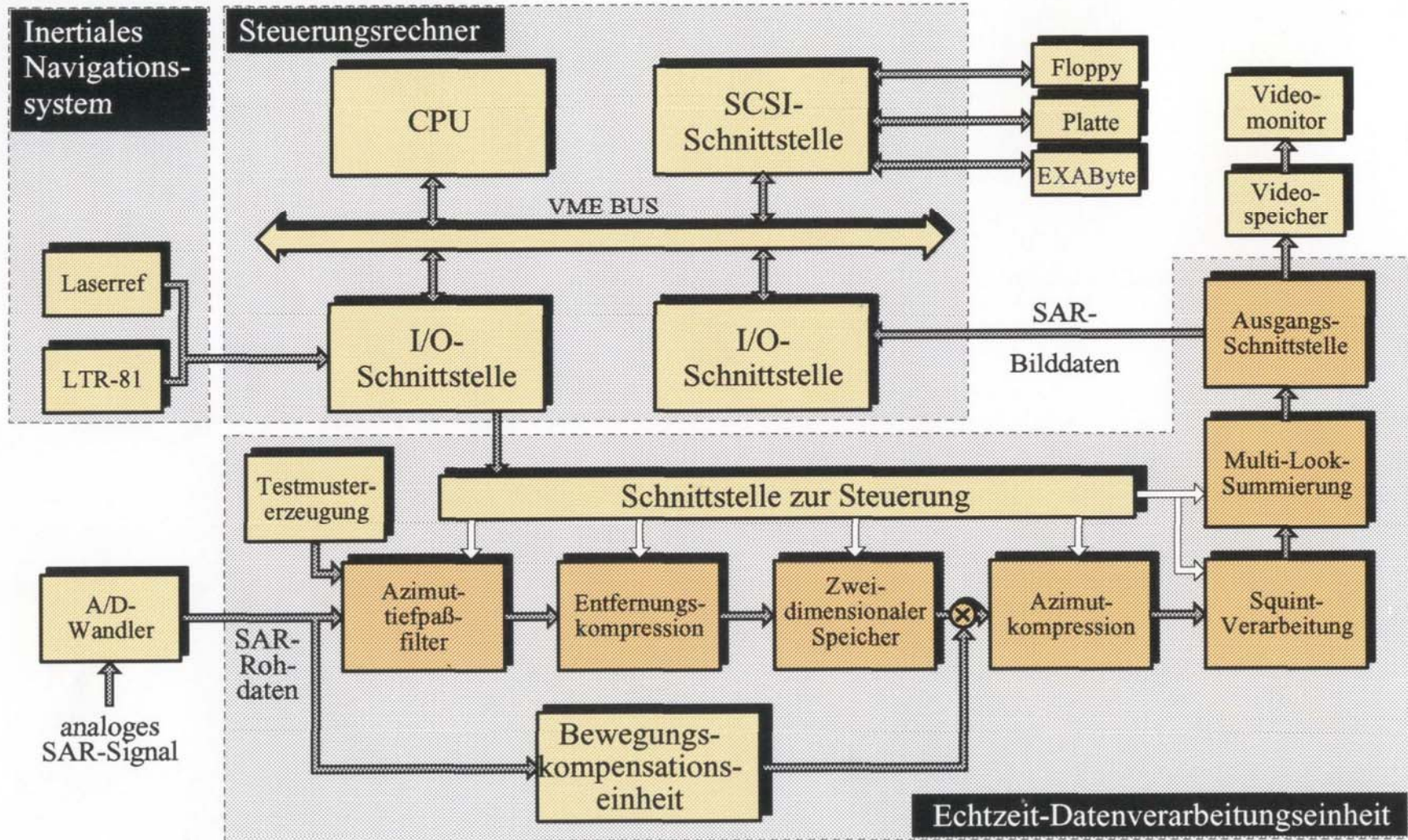
- Einfügung einer Überlappung



Blockdiagramm



- Verarbeitung besteht aus einer kohärenten Summierung von unfokussierten Subaperturen



Blockdiagramm des Echtzeit-SAR-Prozessors

Spezifikationen des Echtzeitprozessors

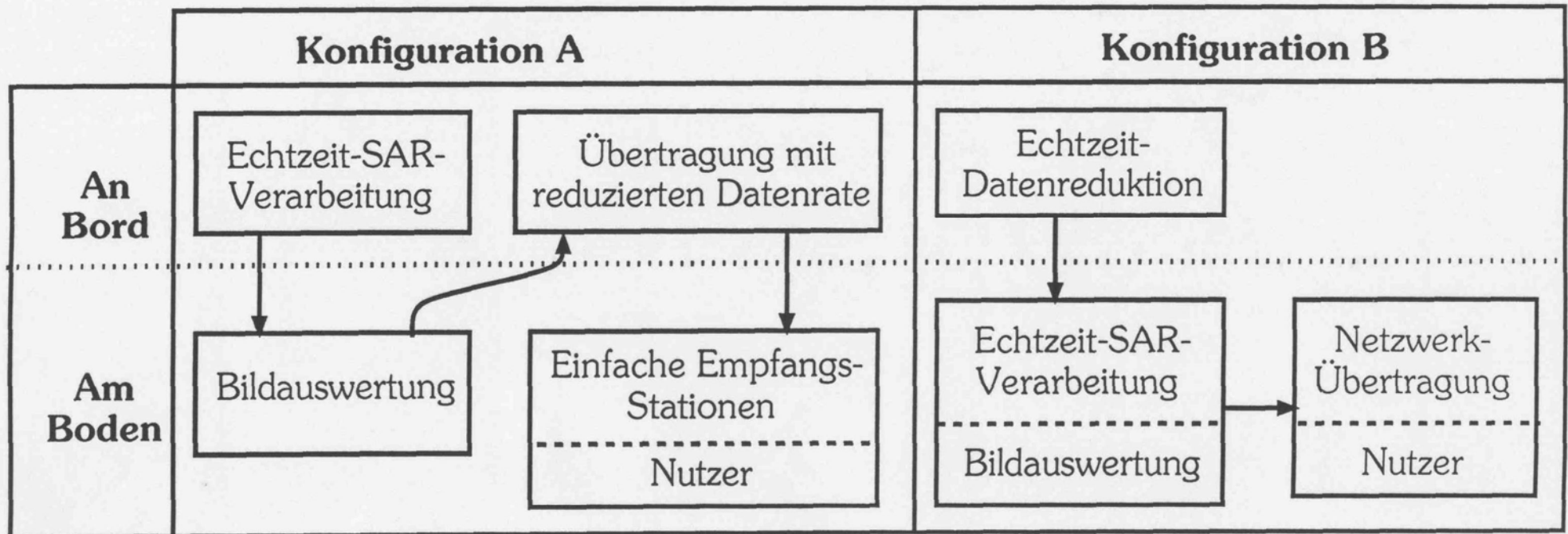
Frequenzband	P	L	C	X
Azimutauflösung [m]	16	3	3	3
Entfernungsauflösung [m]	18	3	2.7	2.7
Anzahl von "Looks"	6	2.7	6.6	8.2
Azimutbandbreite [Hz]	31	62	125	150
Entfernungsbandbreite [MHz]	18	100	100	100

Verarbeitungsparameter

Parameter	Minimum	Typisch	Maximum
Geschwindigkeit [m/s]	50	70	300
Kleinste Entfernung [m]	1500	3000	9000
Größte Entfernung [m]	-	-	40000
PRF [Hz]	660	1000	1240

Ausblick

- Hochauflösende Echtzeit-SAR-Verarbeitung :
 - für Flugzeug-SAR-Systeme ist möglich
 - für satellitengestütztes SAR-Systeme ist zur Zeit nicht möglich
- Datenkompression an Bord ist für SAR-Rohdaten möglich
- Konfigurationen für ein zukünftiges SAR-System mit Echtzeit-Verarbeitung :

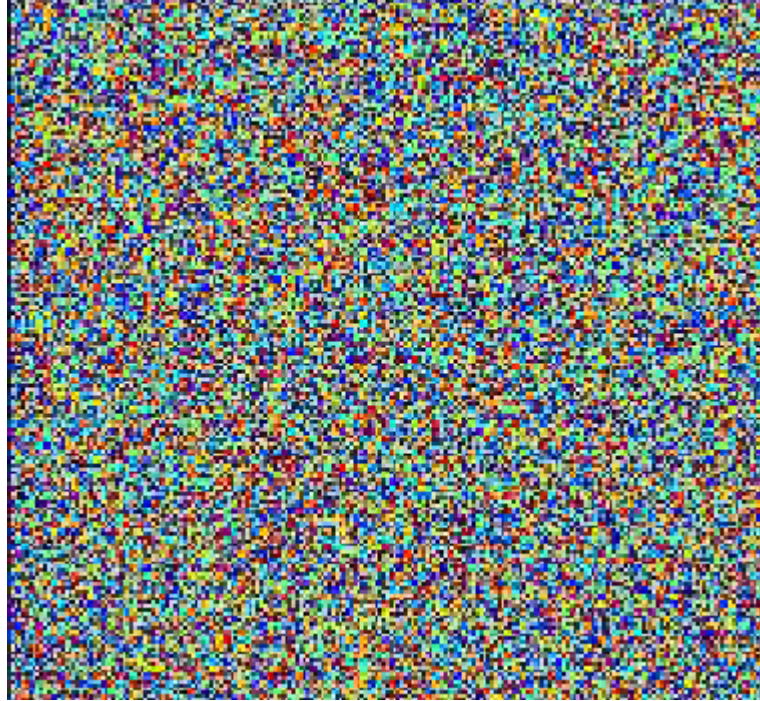


SAR Image

Amplitude



Phase



X-SAR/SIR-C, Mount Etna,

Depth of Focus (DOF)

Defines Nr. of Reference Functions required over the Whole Swath

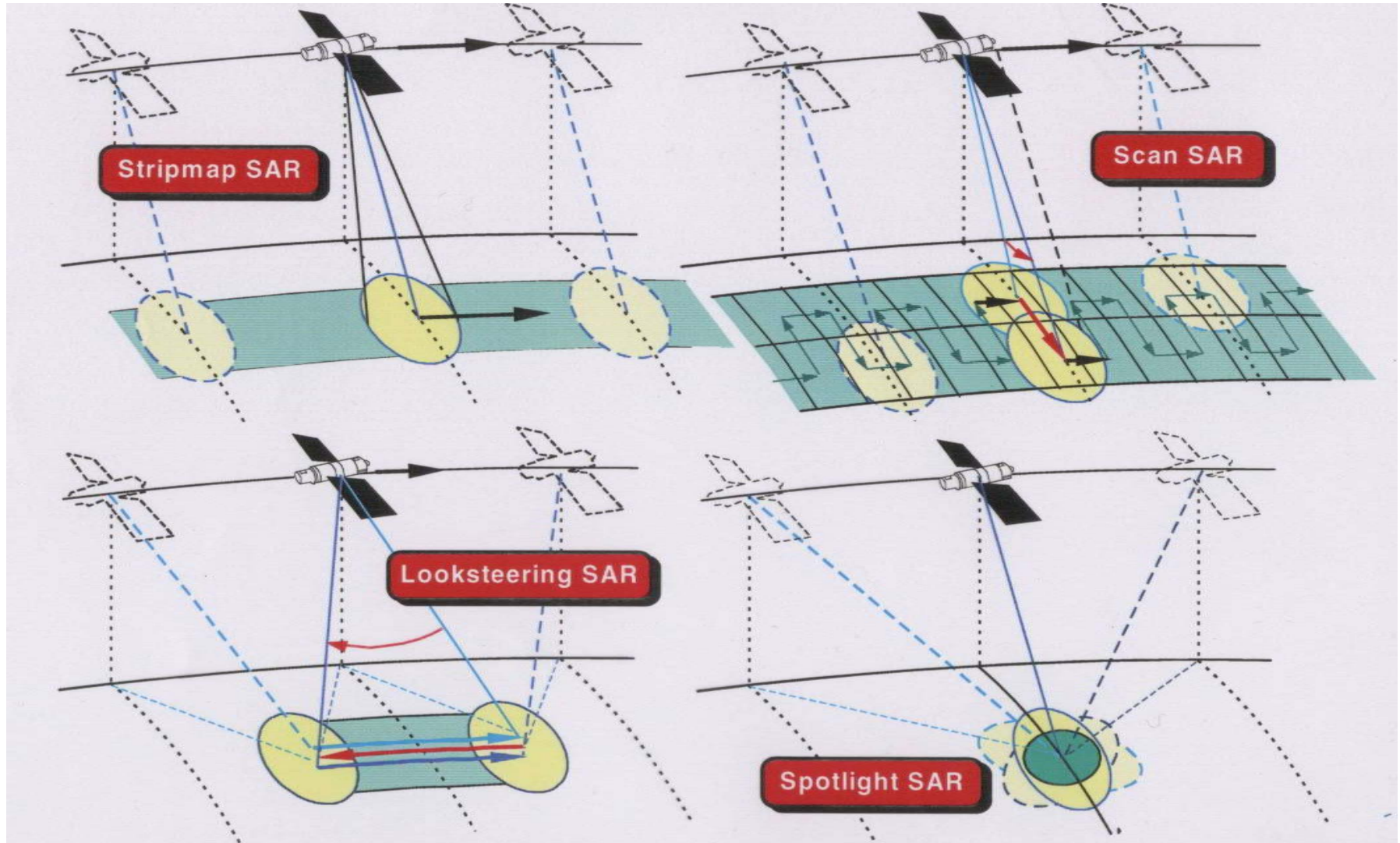
Definition: DoF = $2\Delta r_0$

Required **Accuracy** to match a given quadratic Phase Reference Function to the considered Range for Maximum allowed Phase Error **$|\Delta r - \Delta r_0| = \lambda/8$**

$$r^2 = r_0^2 + \left(\frac{L_s}{2}\right)^2 \rightarrow \frac{dr}{dr_0} = 2r \frac{dr}{dr_0} = 2r_0 \rightarrow \frac{\Delta r}{\Delta r_0} = \frac{r_0}{\sqrt{r_0^2 + \left(\frac{L_s}{2}\right)^2}} \approx 1 - \frac{1}{8} \frac{L_s^2}{r_0^2}$$

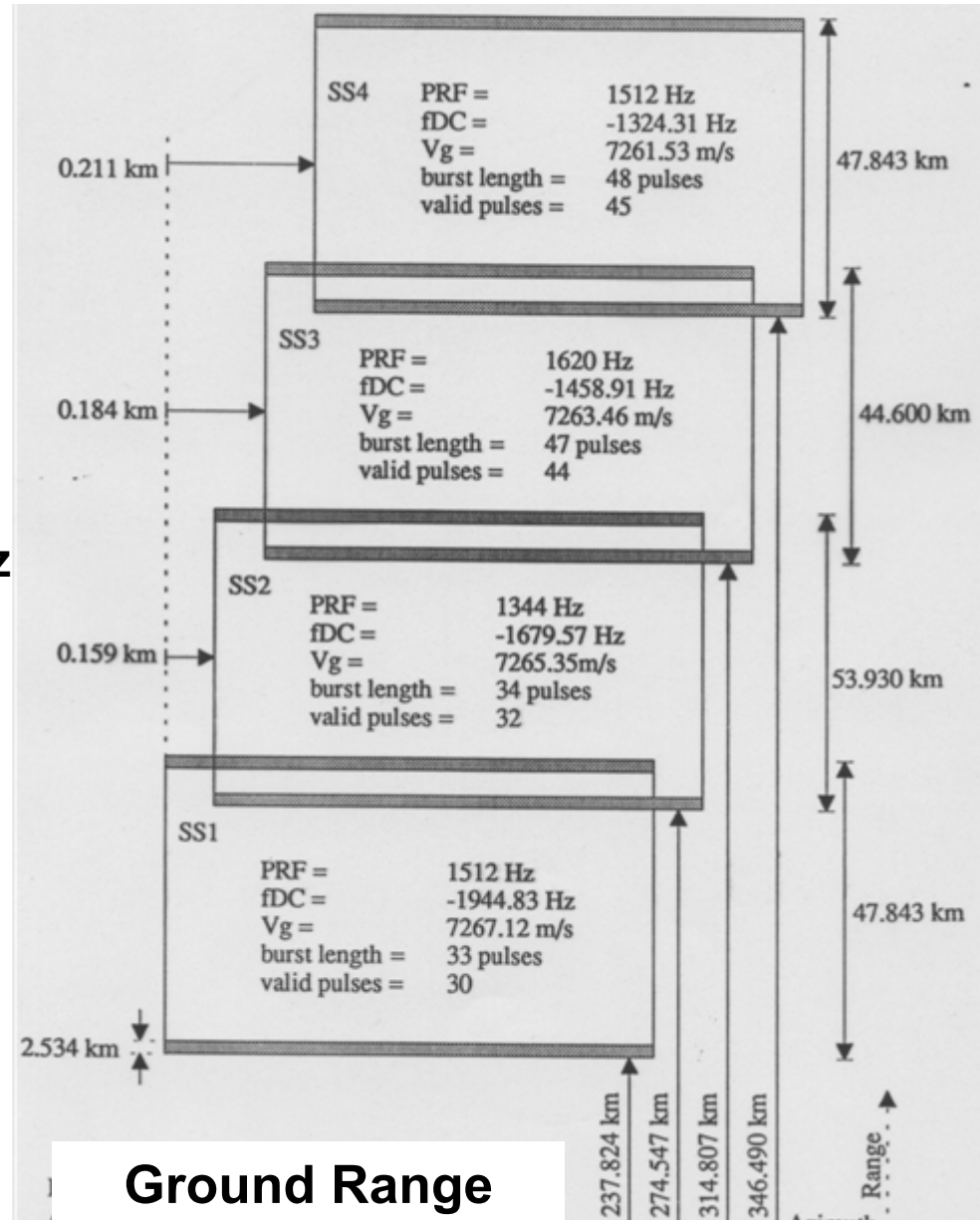
$$|\Delta r - \Delta r_0| = \Delta r_0 \frac{L_s^2}{2(2r_0)^2} = \frac{\lambda}{8}$$

Special SAR Modes



SIR-C ScanSAR, Basic Geometry & Parameter, L-Band

Range Chirp Length 380 Samples
Altitude 2221,009 km
Wavelength 23,9 cm
Sampling Rate 11,24928 MHz



Spotlight versus Stripmap



**Stripmap image
3 m azimuth resolution**



**Spotlight image
0.46 m azimuth resolution**

SAR: Future Developments

- Higher resolution SAR systems (polarimetric, multi-frequency etc)
- Cheaper and more effective T/R-modules
- Geo-stationary transmitter with large deployable antennas and bi-static SAR receivers
- Parasitic SAR Systems (use of signals of opportunity like DTV, GPS)
- New imaging modes (polarimetric interferometry, forward looking, tomography)
- MiniSAR concepts (e.g. Cartwheel)
- Reliable retrieval of geo-physical parameters (development of inverse modeling)
- Alternative platforms (e.g. Zeppelin)
- Commercialization of SAR data (e.g. TerraSAR)
- Symbiotic use of earth observation with communication and navigation (EO/NAV/COM)



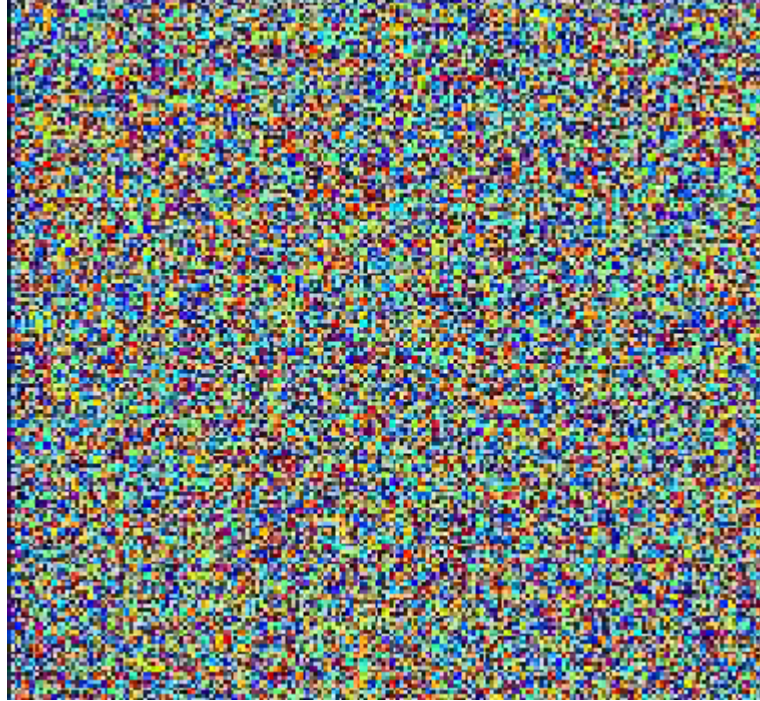
X-Band Image of Munich, E-SAR System

SAR Image

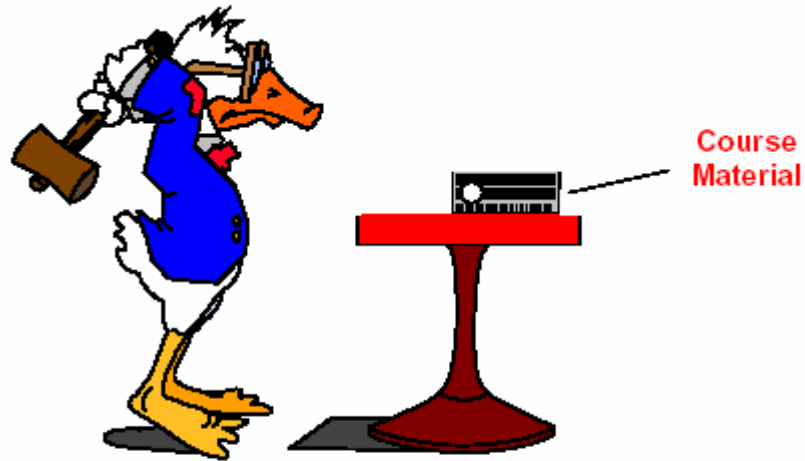
Amplitude



Phase



X-SAR/SIR-C, Mount Etna,



Don't do it !

References I

Carrara, W. et al: Spotlight Synthetic Aperture Radar: Signal Processing Algorithms. Boston: Artech, 1995.

Cook, C., Bernfeld, M.: Radar Signals, An Introduction to Theory and Applications. New York: Academic Press, 1977.

Curlander, J.C., McDonough, R.N.: Synthetic Aperture Radar: Systems and Signal Processing. New York: Wiley, 1991.

Elachi, C.: Spaceborne Radar Remote Sensing: Applications and Technology. New York: IEEE Press, 1988.

Fitch, J. P.: Synthetic Aperture Radar. Springer-Verlag, New York, 1988.

Franceschetti G. und R. Lanari.: Synthetic Aperture Radar Processing. CRC Press, USA, 1999.

Goodman, J. W.: Some Fundamental Properties of Speckle. In: J.Opt. Soc. Am., Vol. 66, No. 11, Nov. 1976, S. 1145-1150.

Harris, F. J.: On the Use of Windows for Harmonic Analysis with the Discret Fourier Transform. In: IEEE Proc., Vol. 66, No. 1, Jan. 1978, S. 51-83.

Hounam, D.: Motion Errors and Compensation Possibilities, in AGARD Lecture Series 182; Fundamentals and special problems of Synthetic Aperture Radar (SAR), August 1992, published by AGARD, ISBN 92-835-0683-9, pp.3-1 to 3-12

References II

Henderson, F. und Lewis, A.: Manual of Remote Sensing: Principles and Applications of Imaging Radar. New York: John Wiley & Sons, 1998.

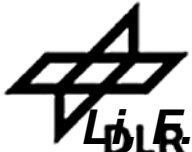
Keydel, W. (Editor): AGARD Lecture Series 182; Fundamentals and special problems of Synthetic Aperture Radar (SAR), August 1992, published by AGARD, ISBN 92-835-0683-9

Keydel, W.: Basic Principles of SAR, in AGARD Lecture Series 182; Fundamentals and special problems of Synthetic Aperture Radar,. (SAR), August 1992, published by AGARD, ISBN 92-835-0683-9, p.p. 1-1 to 1-13

Keydel, W.: SAR Peculiarities, Ambiguities, and Constraints, AGARD Lecture Series 182; Fundamentals and special problems of Synthetic Aperture Radar (SAR), pp.2-1 to 2-10 August 1992, published by AGARD, ISBN 92-835-0683-9, pp.2-1 to 2-10

Kramer, H.J.: Observation of the Earth and its Environment - Survey of Missions and Sensors, Springer, 1996.

Klauder, J.R. et al: The Theory and Design of Chirp Radars. The Bell System Technical Journal, July 1960, S. 745-808.



References III

Li, F.K., Held, D.N., Curlander, J.C., Wu, C.: Doppler Parameter Estimation for Spaceborne Synthetic-Aperture Radars. In: IEEE Trans. Geoscience and Remote Sensing, Vol. 23, No. 1, Jan. 1985.

Li, F.K., Jonson, T.K.: Ambiguities in Spaceborne Synthetic Aperture Radar Systems. In: IEEE Trans. Aerosp. Electron. Syst., Vol. 19, No. 3, Mai 1983, S. 389-397.

Li, F.K., Croft, C., Held, D.: Comparison of Several Techniques to Obtain Multiple-Look SAR Imagery. In: IEEE Trans. Geoscience and Remote Sensing, Vol. 21, No. 3, Juli 1983.

McDonough, R.N. et al: Image Formation from Spaceborne Synthetic Aperture Radar Signals. Johns Hopkins APL Technical Digest, Vol. 6, No. 4, 1985, S. 300-312.

Mittermayer, J., A. Moreira und O. Loffeld: Spotlight SAR Data Processing Using the Frequency Scaling Algorithm. In: IEEE Trans. Geoscience and Remote Sensing, Vol. 37, 1999, S. 2198-2214.

Moreira, A.: Improved Multilook Techniques Applied to SAR and ScanSAR Imagery. In: IEEE Trans. Geoscience and Remote Sensing, Vol. 29, No. 4, 1991.

Moreira, A.: Suppressing the Azimuth Ambiguities in Synthetic Aperture Radar Images. IEEE Trans. Geosci. Remote Sensing, Vol. 31, No. 4, 1993.

Moreira, A., Mittermayer, J., Scheiber, R.: Extended Chirp Scaling Algorithm for Air- and Spaceborne SAR Data Processing in Stripmap and ScanSAR Imaging Modes. In: IEEE Trans. Geoscience and Remote Sensing, Vol. 34, No. 5, 1996.

References IV

Moreira, A.: Radar mit synthetischer Apertur. In: Radar mit realer und synthetischer Apertur, Kapitel 8, Munich:Oldenbourg Verlag, 1999.

Oliver, C. und S. Quegan. Understanding Synthetic Aperture Radar Images. Artech House, 1998.

Raney, R. K.: Theory and Measure of Certain Image Norms in SAR. IEEE Trans. Geosci. Remote Sensing, Vol.23, No.3, Mai 1985.

Raney, R. K. und Wessels, G. J.: Spatial Considerations in SAR Speckle Simulation. IEEE Trans. Geosci. Remote Sensing, Vol. 26, No. 5, Sept. 1988, S. 666-672.

Scheiber, R.: Single-Pass Interferometry with the E-SAR System of DLR. In: Proc. EUSAR Conference, Friedrichshafen, Mai 1998.

Tomiyasu, K.: Tutorial Review of Synthetic-Aperture Radar (SAR) with Applications to Imaging of the OceanSurface. In: IEEE Proc., Vol. 66, No. 5, Mai 1978.

Tomiyasu, K.: Conceptual Performance of a Satellite Borne, Wide Swath Synthetic Aperture Radar. In: IEEE Trans. Geoscience and Remote Sensing, Vol. 19, No. 2, April 1981, S. 108-116.